Atmos. Meas. Tech. Discuss., 8, 935–985, 2015
www.atmos-meas-tech-discuss.net/8/935/2015/
doi:10.5194/amtd-8-935-2015

Atmospheric Measurement Techniques Discussions
Open Access

Tropospheric nitrogen dioxide column retrieval from ground-based zenith-sky DOAS observations

F. Tack[1], F. Hendrick[1], F. Goutail[2], C. Fayt[1], A. Merlaud[1], G. Pinardi[1], C. Hermans[1], J.-P. Pommereau[2], and M. Van Roozendael[1]

[1]BIRA-IASB, Belgian Institute for Space Aeronomy, Brussels, Belgium
[2]LATMOS, Laboratoire Atmosphères, Milieux, Observations Spatiales, Guyancourt, France

Received: 22 December 2014 – Accepted: 9 January 2015 – Published: 26 January 2015

Correspondence to: F. Tack (frederik.tack@aeronomie.be)

Published by Copernicus Publications on behalf of the European Geosciences Union.

Tropospheric NO_2 column retrieval from ground-based zenith-sky DOAS observations

F. Tack et al.

AMTD
8, 935–985, 2015

Tropospheric NO_2 column retrieval from ground-based zenith-sky DOAS observations

F. Tack et al.

Abstract

We present an algorithm for retrieving tropospheric nitrogen dioxide (NO_2) vertical column densities (VCDs) from ground-based zenith-sky (ZS) measurements of scattered sunlight. The method is based on a four-step approach consisting of (1) the Differential Optical Absorption Spectroscopy (DOAS) analysis of ZS radiance spectra using a fixed reference spectrum corresponding to low NO_2 absorption, (2) the determination of the residual amount in the reference spectrum using a Langley-plot-type method, (3) the removal of the stratospheric content from the daytime total measured slant column based on stratospheric VCDs measured at sunrise and sunset, and simulation of the rapid NO_2 diurnal variation, (4) the retrieval of tropospheric VCDs by dividing the resulting tropospheric slant columns by appropriate air mass factors (AMFs). These steps are fully characterized and recommendations are given for each of them. The retrieval algorithm is applied on a ZS dataset acquired with a Multi-AXis (MAX-) DOAS instrument during the Cabauw (51.97° N, 4.93° E, sea level) Intercomparison campaign for Nitrogen Dioxide measuring Instruments (CINDI) held from the 10 June to the 21 July 2009 in the Netherlands. A median value of 7.9×10^{15} molec cm^{-2} is found for the retrieved tropospheric NO_2 VCDs, with maxima up to 6.0×10^{16} molec cm^{-2}. The error budget assessment indicates that the overall error σ_{TVCD} on the column values is less than 28 %. In case of low tropospheric contribution, σ_{TVCD} is estimated to be around 39 % and is dominated by uncertainties in the determination of the residual amount in the reference spectrum. For strong tropospheric pollution events, σ_{TVCD} drops to approximately 22 % with the largest uncertainties on the determination of the stratospheric NO_2 abundance and tropospheric AMFs. The tropospheric VCD amounts derived from ZS observations are compared to VCDs retrieved from off-axis and direct-sun measurements of the same MAX-DOAS instrument as well as to data from a co-located Système d'Analyse par Observations Zénithales (SAOZ) spectrometer. The retrieved tropospheric VCDs are in good agreement with the different datasets with correlation coefficients and slopes close to or larger than 0.9. The potential of the presented ZS

retrieval algorithm is further demonstrated by its successful application on a 2 year dataset, acquired at the NDACC (Network for the Detection of Atmospheric Composition Change) station Observatoire de Haute Provence (OHP; Southern France).

1 Introduction

Nitrogen dioxide (NO_2) is an atmospheric trace gas that plays a major role in atmospheric chemistry (Crutzen, 1979). In the troposphere, it is a key precursor in the formation of ozone (Crutzen, 1970) and aerosols (Chan et al., 2010), and can contribute locally to radiative forcing (Solomon et al., 1999), through which it indirectly affects the climate system. As tropospheric NO_2 abundances mostly coincide with a range of other pollutants it can be seen as a proxy for air pollution in general. According to a recent study on air pollution published by the World Health Organization (WHO, 2013), NO_2 can have a direct impact on human health, causing inflammation, airway hyperresponsiveness and lung cell changes in the short term and respiratory and cardiovascular mortality in the long term. Main sources of tropospheric NO_2 can be of anthropogenic origin, e.g. industrial burning processes and fossil fuel combustion, and natural origin, e.g. lightning and soil emissions. Tropospheric NO_2 concentrations can be highly variable in time and space in polluted regions. For the reasons stated, the long-term and accurate monitoring of this trace gas is of great relevance.

Here, we present a retrieval algorithm developed at BIRA-IASB for deriving tropospheric NO_2 vertical column densities (VCDs) from ground-based (GB) zenith-sky (ZS) observations of scattered sunlight by application of the differential optical absorption spectroscopy (DOAS) technique. DOAS is a well-established remote sensing technique that is able to quantify the abundance of trace gases like NO_2 in the atmosphere, based on their unique spectral signature (Platt and Stutz, 2008). The main principles of the DOAS technique are (1) to separate in the measured scattered sunlight spectra, the fine-scale absorption features of trace gases from broad-band absorption due to scattering effects (mainly Rayleigh and Mie scattering), (2) to analyse the remaining

AMTD
8, 935–985, 2015

Tropospheric NO_2 column retrieval from ground-based zenith-sky DOAS observations

F. Tack et al.

absorber narrow-band structures by least-squares spectral fitting on laboratory cross-sections. The mathematical and physical fundamentals of the method are extensively described in Platt (1994), and Platt and Stutz (2008). DOAS instruments typically operate in the ultraviolet (UV) and visible (Vis) channels of the solar spectrum. In case of the GB ZS-DOAS setup, an optical head, connected to a spectrometer coupled to a charge-coupled device (CCD) detector, points permanently to the zenith. This setup exploits the diurnal variation of the solar zenith angle (SZA).

Many studies can be found in the literature discussing the application of the DOAS method for determination of NO_2 column abundances in the atmosphere based on observations from ground-based, airborne and spaceborne platforms. Without the intention to be complete, an overview of some relevant studies is provided here. The pioneering works of Brewer et al. (1973) and Noxon (1975) report on observations of NO_2 concentrations in the atmosphere based on GB ZS measurements. Since more than three decades, these measurements have been commonly performed to monitor trace gases related to the ozone depletion in the stratosphere, such as NO_2 (e.g. Solomon et al., 1987; McKenzie et al., 1991; Goutail et al., 1994; Hendrick et al., 2004; Denis et al., 2005). More recently, GB Multi-Axis DOAS (MAX-DOAS) has proven to be a suitable and reliable approach to retrieve integrated column amounts of tropospheric trace gases as well as information on their vertical distribution (e.g. Hönninger et al., 2004; Wittrock et al., 2004; Frieß et al., 2006; Clémer et al., 2010; Vlemmix et al., 2011; Wagner et al., 2011; Hendrick et al., 2014). In addition to ZS observations, the GB MAX-DOAS setup measures scattered sunlight from multiple viewing angles towards the horizon (the so-called off-axis geometry), increasing therefore the sensitivity to absorbers present close to the ground, because of the longer light paths through the lower troposphere. The DOAS method is also applied to assess total and tropospheric NO_2 columns from nadir-viewing spaceborne sensors like SCIAMACHY (Scanning Imaging Absorption Chartography), GOME (Global Ozone Monitoring Experiment), GOME-2, and OMI (Ozone Monitoring Experiment) (see e.g. Richter and Burrows, 2002; Beirle et al., 2010; Boersma et al., 2011; Hilboll et al., 2011; Valks

AMTD
8, 935–985, 2015

et al., 2011; Bucsela et al., 2013). Other experiments have been published, presenting approaches to monitor tropospheric NO_2 from car (Johansson et al., 2009; Wagner et al., 2010; Constantin et al., 2013) and airborne platforms (Berg et al., 2012; Merlaud et al., 2012; Popp et al., 2012).

Here we describe the different steps of a new ZS retrieval algorithm for tropospheric NO_2 columns. The limitations and possible alternatives for this method are additionally discussed. Although the sensitivity of ZS-DOAS observations to tropospheric NO_2 is lower compared to MAX-DOAS observations, the presented approach offers new perspectives for the exploitation of ZS UV-Vis measurements, especially the historical time series of such observations performed over the last two decades in the framework of NDACC (Network for the Detection of Atmospheric Composition Change). So far, only a few studies have been published focusing on the retrieval of tropospheric NO_2 column amounts solely based on GB ZS-DOAS observations. Chen et al. (2009) presented a retrieval algorithm, applied on ZS observations acquired in Shanghai (China). There are, however, a number of methodological differences with the approach presented here and these will be further discussed in this paper. In Dieudonné et al. (2013), a similar method is applied on ZS observations acquired in Paris (France). However, the retrieval strategy is discussed only very briefly as the focus of the latter publication is on linking retrieved tropospheric NO_2 columns to surface concentrations.

The organization of this paper is as follows: Sect. 2 is dedicated to the description of the GB instrument used for the ZS observations, as well as the site where measurements were conducted. Section 3 describes the four main steps of the developed methodology for tropospheric NO_2 VCD retrieval from GB ZS-DOAS observations. Furthermore, the four steps of the retrieval approach are characterised in terms of an error budget analysis. Section 4 presents the retrieval results, including a comparison with correlative MAX-DOAS, direct sun (DS-) DOAS, and SAOZ (Système d'Analyse par Observations Zénithales) data. Section 5 discusses the retrieval approach with a focus on recommendations for application of the method on ZS observations at other stations. In Sect. 6 the application on observations acquired over two years at the NDACC

AMTD
8, 935–985, 2015

site of Observatoire de Haute Provence (OHP; Southern France) is demonstrated. The paper concludes with a brief summary.

2 Ground-based DOAS observations

The retrieval algorithm is first tested on a dataset acquired from the 10 June to the 21 July 2009 by the BIRA-IASB MAX-DOAS instrument operated in the framework of the international Cabauw Intercomparison campaign for Nitrogen Dioxide measuring Instruments (CINDI). The CINDI campaign took place at Cabauw, the Netherlands (51.97° N, 4.93° E, sea level) at the Cabauw Experimental Site for Atmospheric Research (CESAR; http://www.cesar-observatory.nl). It is located in a semi-rural area in the direct proximity of the four largest cities of the Netherlands (i.e. Amsterdam, Rotterdam, Den Haag and Utrecht). One of the main objectives of the campaign was to intercompare and intercalibrate GB instruments measuring NO_2 and determine their performance and accuracy. A more in-depth discussion of the CINDI campaign and results can be found in Roscoe et al. (2010) and Piters et al. (2012).

The BIRA-IASB MAX-DOAS instrument consists of three main parts. The optical head, mounted on a suntracker (INTRA manufactured by Brusag), can collect the scattered sunlight over a wide range of elevation (0 to 90°) and azimuth angles (0 to 360°). Optical fibers guide the collected skylight from the output of the optical head to the spectrometers, the latter being placed in a thermo-regulated container to guarantee high stability and minimise thermal stress. The dual-channel system is composed of a UV (ORIEL model MS260i; 1200 grooves mm^{-1} grating) and a visible (ORIEL model MS127; 600 grooves mm^{-1}) grating spectrometer covering a wavelength range of 300–390 nm and 400–720 nm, respectively. The Gaussian shaped instrument's slit function has a spectral resolution of 0.4 nm full width at half maximum (FWHM) and 0.9 nm FWHM for the UV and visible channels, respectively. Both spectrometers are connected to low-noise thermo-electrically cooled CCD detectors (Princeton Instruments, model PIXIS 2KBUV with 2048 × 512 pixels for the UV channel and Princeton Instruments,

AMTD
8, 935–985, 2015

model Spec-10: 100B with 1340 × 100 for the visible channel). A pc unit controls the acquisition and stores all the measured spectral data. The data acquisition is fully automated using a software developed at BIRA-IASB. A full description of the instrument can be found in Clémer et al. (2010). The configuration of the instrument allows to measure scattered sunlight from ZS and off-axis viewing angles, as well as to perform DS observations. Each complete MAX-DOAS scan takes approximately 20 min and comprises ten different elevation angles, including ZS observations.

3 Tropospheric NO_2 vertical column retrieval algorithm

The developed methodology for tropospheric NO_2 vertical column retrieval from GB ZS-DOAS observations of scattered sunlight is based on a four-step approach. An overview of the approach is given here while the different steps are described in detail in the following subsections. First, the ZS spectra are analysed by the DOAS spectral fitting (see Sect. 3.1). The direct output of the DOAS analysis is the differential slant column density (DSCD), which is the concentration of the trace gas of interest integrated along the effective light path with respect to a fixed amount of the same absorber in a measured reference spectrum. As many light paths contribute in case of scattered sunlight observations, the measured slant column is a weighted average over all contributions. Air mass factors are calculated in order to model radiative transfer in the atmosphere and to convert slant columns to vertical columns (see Sect. 3.2). Ideally, the concentration of the absorber in the background spectrum should be zero. However, usually it contains low absorption from the measured species itself and therefore the residual amount in the reference spectrum (RSCD) needs to be determined accurately in order to realize the conversion from the DSCD to the total measured slant column density (MSCD) (see Sect. 3.3):

$$\text{MSCD} = \text{DSCD} + \text{RSCD} \quad (1)$$

Discussion Paper | Discussion Paper | Discussion Paper | Discussion Paper |
AMTD
8, 935–985, 2015
Tropospheric NO_2 column retrieval from ground-based zenith-sky DOAS observations
F. Tack et al.

In the next step, the stratospheric slant column density (SSCD) is determined and removed from the total slant column in order to derive the tropospheric slant column density (TSCD) (see Sect. 3.4):

$$\mathrm{TSCD} = \mathrm{MSCD} - \mathrm{SSCD} \tag{2}$$

In the final step, TSCDs are converted to tropospheric vertical column densities (TVCDs) by using appropriate tropospheric air mass factors (TAMFs) (see Sect. 3.5):

$$\mathrm{TVCD} = \frac{\mathrm{TSCD}}{\mathrm{TAMF}} \tag{3}$$

3.1 DOAS analysis of zenith radiance spectra

The ZS observations of scattered sunlight are analysed by the QDOAS spectral fitting tool, developed at BIRA-IASB (Danckaert et al., 2014). The 425–490 nm visible wavelength region is used, as NO_2 is characterised by strongly structured absorption lines in this fitting window enhancing the sensitivity to the absorber, while on the other hand interference with the spectral signature of other absorbers is minimised in this spectral region. In addition to the relevant trace gas cross-sections (NO_2, O_3, H_2O, O_4), also a synthetic Ring spectrum and a low-order polynomial term are included into the non-linear least-squares fitting. They account for respectively the Ring effect (Grainger and Ring, 1962), i.e. the filling-in of Fraunhofer lines, and the contribution of broad-band absorption and scattering effects (mainly Rayleigh and Mie scattering).

The main DOAS settings used in this study as well as the cross-sections included in the spectral fit are given in Table 1. They have been chosen in accordance with the recommendations made by the NDACC UV-Vis Working Group for the sake of harmonising the different datasets provided to the NDACC database (Van Roozendael and Hendrick, 2012).

DSCDs are the direct output of the QDOAS spectral fitting approach. Prior to further analysis, the NO_2 DSCDs are quality-checked based on: (1) their uncertainty, expressed as SD, and (2) the residual structure of the retrieval fit, expressed as root

AMTD
8, 935–985, 2015

mean square error (RMS). Both measures of dispersion, which can be interpreted as quality flags for the measurements, are calculated for each DSCD by the QDOAS software. An empirically derived threshold based on the 95 % confidence interval is set for both parameters to determine whether or not a measurement is an outlier, e.g. due to low SNR, and needs to be rejected. On a total of 4226 DSCDs retrieved based on ZS-DOAS observations, 128 were rejected after the quality check.

Beside NO_2 DSCDs, also the oxygen dimer (O_4) DSCDs have been retrieved. They are essential to determine the presence of aerosols and clouds, which can both affect the tropospheric NO_2 retrieval. O_4 has a well-known and nearly constant column and vertical distribution in the atmosphere, mainly depending on temperature and pressure, and thus on the altitude. This makes the oxygen dimer highly sensitive to the variation of scattering due to aerosols and clouds, and therefore useful to derive information on these parameters, as discussed in Wagner et al. (2004) and Frieß et al. (2006). A high aerosol loading and/or tropospheric clouds can introduce additional multiple scattering, which can significantly enhance the light path, and subsequently the measured NO_2 optical depth. This results in an overestimation of the "true" NO_2 amount. The retrieved NO_2 differential slant columns are screened for this effect according to the following approach: the O_4 diurnal variation is first modeled with the atmospheric radiative transfer model (RTM) UVspec/DISORT (Mayer and Kylling, 2006) and the AFGL standard atmosphere, and then compared with the retrieved O_4 slant columns. The nearly constant concentration of O_4 in the atmosphere results in a diurnal variation characterised by a slow increase at higher SZAs, and therefore by a smooth u-shaped curve in case of a clear and non-polluted day. An empirically derived threshold is set to determine significant offsets from the modeled O_4, indicating a high aerosol loading and/or the presence of clouds introducing multiple scattering. When this threshold is exceeded, the corresponding NO_2 DSCD spike is identified and rejected. Without the application of the aforementioned filter strategy, a number of outliers could be observed when comparing the retrieved tropospheric NO_2 VCD time series with reference data. For example for day 187 (6 July 2009), such an NO_2 enhancement event could be observed, as shown in Fig. 1.

3.2 Air mass factors

Multiple unknown light paths of scattered sunlight contribute simultaneously to the measured ZS signal. To quantify an effective light path and thus to be able to interpret the observations, radiative transfer in the atmosphere needs to be modeled. Generally the optical path is not expressed in absolute units, e.g. meters, but in terms of an AMF (Solomon et al., 1987), being the ratio of the number of molecules per cm^2 detected in an observation (SCD) and the integrated amount of molecules per cm^2 expected for a single, vertical transect of the atmosphere (VCD):

$$\mathrm{AMF} = \frac{\mathrm{SCD}}{\mathrm{VCD}} \tag{4}$$

AMFs are typically determined by using a radiative transfer model (RTM). It simulates the radiative transfer of electromagnetic radiation through this atmosphere, based on a priori information on the state of the atmosphere (pressure, temperature, absorbers vertical profiles, aerosol loading, cloud cover, and surface albedo). The AMF enhancement factor calculation depends also on the geometry of observation and the position of the sun.

The retrieval approach requires the calculation of stratospheric and tropospheric AMFs (see Sects. 3.4 and 3.5). Equation (4) can be reformulated for the stratosphere and troposphere as follows:

$$\mathrm{SAMF} = \frac{\mathrm{SSCD}}{\mathrm{SVCD}} \tag{5}$$

and

$$\mathrm{TAMF} = \frac{\mathrm{TSCD}}{\mathrm{TVCD}} \tag{6}$$

AMTD
8, 935–985, 2015

3.2.1 Stratospheric AMF

Stratospheric AMFs have been calculated with the RTM package UVspec/DISORT (Mayer and Killing, 2005). This code has been thoroughly validated in the framework of an intercomparison exercise between different RTMs for the interpretation of GB ZS-DOAS and MAX-DOAS observations (Hendrick et al., 2006; Wagner et al., 2007). The radiative transfer equation (RTE) is numerically solved by the discrete ordinate method in a pseudo-spherical geometry and including multiple scattering. The wavelength used here is 457 nm, i.e. the middle of the NO_2 fitting window. Since stratospheric NO_2 is characterised by a strong diurnal variation due to photochemistry, the corresponding changes of the concentration along a given light path complicate the calculation of AMFs, especially at twilight. To account for this effect, the RTM is initialised with NO_2 fields depending on SZA and altitude and generated by a photochemical model. In this study, the stacked box photochemical model PSCBOX (Errera and Fonteyn, 2001; see also Hendrick et al., 2004) is coupled to the RTM UVspec/DISORT. PSCBOX includes 48 variable species, 104 gas-phase and 27 photolysis reactions and is initialised daily with 12:00 UT pressure, temperature, and chemical species profiles from the three-dimensional chemical transport model (3-D CTM) SLIMCAT (Chipperfield, 2006) for the dates and location of interest. Pressure and temperature fields used in SLIMCAT are taken from UKMO (UK Meteorological Office) meteorological analyses. The output time step is 6 min. For the calculation of stratospheric AMFs, UVspec/DISORT parameters for aerosol loading, cloud cover, and surface albedo are respectively set at summer background conditions with a visibility of 20 km, clear-sky, and 0.07. Then, AMFs are interpolated from the calculated NO_2 AMF look-up tables to the date and time/SZA corresponding to the observations.

3.2.2 Tropospheric AMF

In contrast to the stratospheric contribution, tropospheric NO_2 concentrations can be highly variable in time and space in polluted regions. For an optimal simulation of tro-

Discussion Paper | Discussion Paper | Discussion Paper | Discussion Paper |

AMTD

8, 935–985, 2015

Tropospheric NO_2 column retrieval from ground-based zenith-sky DOAS observations

F. Tack et al.

pospheric AMFs, realistic a priori profiles that take into account local pollution events are required. Therefore daily NO_2 and aerosol profiles retrieved from the BIRA-IASB MAX-DOAS observations performed during CINDI have been used to derive appropriate tropospheric NO_2 AMFs. These calculations were done with the bePRO package based on the LIDORT RTM (Spurr, 2008). This RT suite, dedicated to the retrieval of trace gas and aerosol vertical profiles, and AMF calculation, based on the Optimal Estimation Method (Rodgers, 2000), is extensively described in Clémer et al. (2010) and Hendrick et al. (2014). Tropospheric NO_2 AMF look-up tables have been generated for morning and afternoon conditions based on the averaging of the daily AMFs calculated for the CINDI campaign period. For the aerosol and NO_2 vertical profile retrievals, the following settings have been used: altitude grid with ten layers of 200 m thickness between 0 and 2 km, two layers of 500 m between 2 and 3 km, and 1 layer between 3 and 4 km, pressure and temperature profiles from US Standard Atmosphere, and a surface albedo of 0.07, which is the yearly mean value extracted at 440 nm for Cabauw from the Koelemeijer et al. (2003) albedo climatology. Regarding the a priori profiles, an exponentially decreasing profile corresponding to an AOD of 0.05 and a scaling height of 1 km has been chosen for the aerosol retrieval. Aerosol single scattering albedo and phase moments were derived as in Clémer et al. (2010) based on co-located AERONET sun photometer measurements. In the case of NO_2, a profile decreasing linearly from 0.3 ppb at 0 km to 0.01 ppb at 4 km was used as a priori. The a priori covariance matrices for aerosol and NO_2 were constructed as in Clémer et al. (2010). It should be also noted that the stratospheric NO_2 content is removed from the measured DSCDs by taking the zenith measurement of each scan as reference.

3.3 Determination of the residual amount in the reference spectrum

In the DOAS analysis, the concentration of NO_2 is determined with respect to a fixed amount of the absorber in a selected reference spectrum. This method is commonly applied to remove the most prominent structures in the measured spectra, the so-called solar Fraunhofer lines, as they blur out the much weaker absorption structures

AMTD
8, 935–985, 2015

F. Tack et al.

of trace gases. Furthermore, taking the ratio of measured spectra and a Fraunhofer reference spectrum cancels out instrumental effects under the assumption that the characteristics of the instrument remain stable over a sufficiently long period. Usually this background spectrum contains (low) absorption from the measured species itself. This residual amount is, however, unknown and needs to be quantified in order to be able to determine the total measured slant column (see Eq. 1).

It should be mentioned that the concentration of the absorber in the background spectrum would be zero if an observation outside of the Earth's atmosphere could be used. This would avoid the necessity to quantify RSCD. However, as discussed in Herman et al. (2009) accurate matching of an extraterrestrial spectrum measured with a spaceborne instrument to the GB ZS measured spectra has proven to be hard due to the differences between the wavelength-dependent instrument slit functions. Usually an appropriate observation from the GB instrument itself serves as reference. To minimise the NO_2 amount in the background spectrum, the reference is commonly taken on a non-polluted, clear-sky day around local noon, when the sun is high and therefore the atmospheric absorption, especially in the stratosphere, is low. For the analysis of the dataset, a ZS noon spectrum was selected on 21 June 2009 at 12:16 LT (SZA = 29.3°).

To constrain and quantify the residual amount of NO_2 in the reference spectrum, the statistical Minimum-amount Langley-Extrapolation (MLE) method is applied, as described in Herman et al. (2009). The MLE method is based on the assumption that the minimum VCDs are constant or in other words independent from the AMF during a portion of the measurement time. The RSCD can be quantified by plotting the observed DSCDs for the whole dataset in function of the associated AMFs, calculated in Sect. 3.2.1. Based on Eqs. (1) and (4) the relation between these quantities can be formulated as:

$$\mathrm{DSCD} = \mathrm{VCD} \times \mathrm{AMF} - \mathrm{RSCD} \tag{7}$$

AMTD
8, 935–985, 2015

The MLE plot of the observed DSCDs and associated AMFs is given in Fig. 2. To reduce the impact of uncertainties in the calculation of the AMFs, only observations with an AMF below 5 are taken into account in the analysis. This threshold corresponds to an SZA of approximately 80°. The plotted DSCDs are binned in sets of 30 points per group, starting from the lowest to the highest AMF. Then in each bin, the lowest value is identified and selected. Thereafter, a linear regression is applied on the selected minima. According to Eq. (7), the opposite of the y-intercept gives an approximation for the residual amount in the reference spectrum. In the present case, a value of 6.2×10^{15} molec cm^{-2} was determined based on the MLE method. It should be noted that in Chen et al. (2009), the RSCD was determined using a completely different strategy, due to the absence of days without pollution. It was based on measurements performed when the ZS instrument was located in a clean area as close as possible to the polluted site of interest (Shanghai), in combination to co-located long-path DOAS observations.

In principle a single reference spectrum can be used for the analysis of long-term measurements if the instrumental properties stay stable. In case of instrumental instability or configuration changes, a drift or/and a bias could be found in the observations, requiring the determination of additional RSCDs for the periods corresponding to the different instrumental conditions. Instrumental stability can be monitored based on the uncertainty on the NO_2 DSCDs and the RMS on the retrieval fit, both a direct product of the DOAS analysis.

Despite the limitations to quantify the NO_2 RSCD, it should be mentioned that since a single reference is used for the analysis of the whole dataset, potential errors in the RSCD determination will affect all measurements in the same way. Thus, these RSCD errors scarcely affect the relative variation of the retrieved tropospheric VCDs.

3.4 Determination of stratospheric contribution to the total NO_2 column

In order to obtain tropospheric SCDs, stratospheric SCDs need to be removed from the total measured SCDs (see Eq. 2). SSCDs are derived as follows: first, SVCDs

AMTD
8, 935–985, 2015

are retrieved both for 90° SZA sunrise and sunset. Then output from the photochemical box-model PSCBOX is used to extrapolate both the 90° SZA twilight SVCDs to daytime values. Finally the calculated SVCDs are converted to SSCDs based on the corresponding stratospheric AMFs.

3.4.1 Retrieval of stratospheric VCDs at sunrise and sunset

For the retrieval of stratospheric VCDs from ZS observations at twilight, the approach recommended by the NDACC UV-Vis Working Group is followed (Van Roozendael and Hendrick, 2012). It is based on the assumption that in case of ZS observations at dawn and dusk, the effective light path in the stratosphere is significantly longer than in the troposphere. Therefore, the tropospheric content generally does not contribute significantly to the total measured slant column (MSCD). Neglecting the NO_2 tropospheric content, Eq. (5) can be rewritten as:

$$\text{SVCD} = \frac{\text{MSCD}}{\text{SAMF}} \tag{8}$$

Only the twilight observations in a limited SZA range (86–91°) around 90° SZA are taken into account. For both sunrise and sunset, the SVCD is determined by applying a linear regression on the measurements in the above SZA range and by taking the values corresponding to 90° SZA. According to Van Roozendael et al. (1994), the precision and accuracy of the SVCD retrievals are maximized at approximately 90° SZA.

Despite the assumed insignificant sensitivity of twilight observations to the troposphere, tropospheric NO_2 pollution events could still be observed in the measurements for a significant number of days at a place like Cabauw. The strong interference of tropospheric NO_2 pollution hampers the correct retrieval of the stratospheric contribution to the total NO_2 column. More precisely, it induces an overestimation of the stratospheric content. To cope with this problem, an approach is proposed to identify a non-polluted reference day and to assume that the retrieved stratospheric content for this day is representative for the whole dataset, instead of a daily observation of the

AMTD
8, 935–985, 2015

stratospheric NO_2 amount. Various criteria need to be taken into account to evaluate and identify such a suitable reference day:

1. Identification of days with, in general, a low tropospheric NO_2 contribution in the absence of local perturbations caused by tropospheric pollution events. Non-polluted days can be differentiated based on a screening of plots of the NO_2 DSCDs or SCDs as a function of SZA. The diurnal cycle of a "clean" day, dominated by stratospheric absorption, is well-defined and typically has the shape of a smooth u-shape without perturbations (see Fig. 3a).

2. Identification of non-overcast days with low aerosol loading based on plots of the O_4 DSCDs or SCDs. The oxygen dimer is highly sensitive to variation in the aerosol concentration or in the presence of clouds as already discussed in Sect. 3.1. Days with a low aerosol loading typically have a minimal deviation from the modeled O_4 diurnal variation, characterized by a smooth u-shape (see Fig. 3b).

3. Notwithstanding the fact that the DSCDs are already quality-checked in Sect. 3.1, based on the slant error and the RMS on the fit, a reference day should be characterised by low values for both parameters.

4. Preferably a reference day should be selected near to the middle of the dataset in order to minimise the bias, due to the stratospheric NO_2 temporal variance and/or seasonality, between the stratospheric NO_2 content of the reference day and the "true" stratospheric NO_2 content of the other days.

Day 174 (23 June 2009) was selected as the best reference candidate. The corresponding SVCD values are 4.0×10^{15} and 5.8×10^{15} molec cm^{-2} for sunrise and sunset, respectively (see Fig. 4). Although this day does not meet the fourth criterion, no better candidates could be identified due to high tropospheric contamination, high aerosol loading or clouds. Note that the aforementioned selection criteria are solely based on

AMTD
8, 935–985, 2015

the observed spectra itself. According to correlative meteorological observations and in-situ measurements (Piters et al., 2012), day 174 was also identified as a clean, non-overcast day.

Although the temporal variance of the stratospheric NO_2 content can be assumed to be small over a short time interval, it is characterised by a relatively strong seasonality. Therefore, the above approach can be applied for short-term datasets like the CINDI campaign. In the case of long-term observations, especially at mid- and high-latitudes, reference days for stratospheric NO_2 correction should be preferably selected at least every month, or better, on a weekly basis.

3.4.2 Stratospheric NO_2 diurnal variation modeling between sunrise and sunset

Stratospheric NO_2 is characterised by a strong diurnal cycle which depends not only on the scattering geometry but predominantly on the photochemistry, as discussed already in Sect. 3.2.1. During nighttime, O_3 oxidises NO to NO_2 in the absence of sunlight. At sunrise there is a strong decrease of NO_2 due to photolysis. During daytime at mid-latitude, NO_2 displays a near-linear increase due to the slow photolysis of N_2O_5. At sunset a rapid increase of NO_2 occurs due to the progressive absence of photolytic loss.

In this study, the photochemical model PSCBOX described in Sect. 3.2.1 is used to calculate the rapid variation of the NO_2 concentration at twilight. PSCBOX is initialised with output of the 3-D CTM SLIMCAT based on the date of the selected clean reference day. Then, the simulated NO_2 diurnal cycle is made consistent with the observations and fitted on the stratospheric VCDs retrieved at twilight for the reference day: a scaling factor is calculated by taking the ratio of the retrieved and simulated stratospheric VCD at 90° SZA for both sunrise and sunset and it is then interpolated for the SZA range in between. Finally, the full NO_2 diurnal variation is warped on the retrieved stratospheric twilight VCDs by multiplying the simulated NO_2 diurnal cycle by the varying scaling factor. Obtaining the stratospheric NO_2 diurnal cycle by combining measurements and a CTM has the advantage that that the model accounts for dynam-

AMTD
8, 935–985, 2015

ical features in stratospheric NO_2 while the retrieval does not depend quantitatively on the CTM. Instead it is driven by and in good agreement with the observations. The simulated and measurement-adjusted NO_2 VCD diurnal cycles are both illustrated in Fig. 4.

In Chen et al. (2009), an assumption is made that the typical NO_2 diurnal cycle is characterized by a quasi-linear increase and that this can be modeled by a linear interpolation between the retrieved stratospheric NO_2 VCDs at 90° SZA sunrise and sunset. As illustrated in Fig. 4 by the red dotted curve, this assumption is valid between approximately 80° SZA sunrise and sunset. Applying a linear interpolation between 90° SZA sunrise and sunset leads to an overestimation of the stratospheric content by approximately 1.0×10^{15} molec cm^{-2} with respect to the simulated diurnal variation, adjusted with measurements at 90° SZA sunrise and sunset. This point is further discussed in Sect. 3.6.

3.5 Determination of the NO_2 tropospheric vertical column

Once the daytime SVCDs have been converted into SSCDs using Eq. (5), the retrieval of tropospheric NO_2 VCDs is straightforward (see Eqs. 2 and 3): SSCDs are removed from MSCDs and resulting TSCDs are converted into TVCDs using appropriate AMFs from the generated look-up tables (TAMFs; see Sect. 3.2.2). TVCDs are retrieved for each day of the dataset between sunrise and sunset with usually a time interval of approximately 20 min. For a number of days the frequency is significantly lower because of instrumental issues or the removal of observations with a large uncertainty, as it was described in Sect. 3.1. As sensitivity to the troposphere is decreasing fast with larger SZAs, tropospheric columns are derived only during daytime for SZAs below 80°.

Despite the fact that this study focuses on retrieval of tropospheric VCDs, the retrieved daytime SVCDs are also a valuable product of the approach. It should be mentioned, however, that the observed spectra are analysed with a NO_2 cross-section at room temperature (298 K) instead of with a cross-section at 220 K, commonly used for retrieval of stratospheric columns. Therefore, the retrieved SVCD product will be sys-

AMTD
8, 935–985, 2015

tematically overestimated, as described in Vandaele et al. (1998), due to the temperature dependency of the NO_2 cross-section and the fact that the effective stratospheric NO_2 temperature is not taken into account. A compensation factor is applied in order to correct the retrieved SVCDs. This factor, given by the slope of the regression between the "warm" and "cold" cross-sections, is of about 0.8 for the 220–298 K temperature interval.

3.6 Error budget analysis

To assess the tropospheric NO_2 VCD retrieval approach, the main error sources related to the different steps are estimated and discussed here. Based on Eqs. (1)–(3) can be reformulated as:

$$\mathrm{TVCD} = \frac{\mathrm{DSCD} + \mathrm{RSCD} - \mathrm{SSCD}}{\mathrm{TAMF}} \tag{9}$$

The different contributing uncertainties are assumed to be sufficiently uncorrelated with each other as they arise from nearly independent steps. The combined or overall error of the different identifiable uncertainty sources of the tropospheric NO_2 VCD retrieval approach can then be calculated by using the following error propagation method:

$$\sigma^2_{\mathrm{TVCD}} = \left(\frac{\sigma_{\mathrm{DSCD}}}{\mathrm{TAMF}}\right)^2 + \left(\frac{\sigma_{\mathrm{RSCD}}}{\mathrm{TAMF}}\right)^2 + \left(\frac{\sigma_{\mathrm{SSCD}}}{\mathrm{TAMF}}\right)^2 + \left(\frac{\mathrm{TSCD}}{\mathrm{TAMF}^2} \times \sigma_{\mathrm{TAMF}}\right)^2 \tag{10}$$

Four main error sources are contributing to the overall uncertainty on the retrieved NO_2 TVCDs: (1) random errors caused by noise in the spectral measurements and the DOAS spectral fitting (σ_{DSCD}), (2) errors originating from the estimation of the NO_2 SCD residual amount in the reference spectrum (σ_{RSCD}), (3) errors related to the estimation of the stratospheric contribution to the total NO_2 column (σ_{SSCD}), and (4) errors in the calculation of the tropospheric AMFs (σ_{TAMF}) caused by the uncertainties due to the assumptions made for the NO_2 profile shape, aerosol effects and surface albedo.

AMTD
8, 935–985, 2015

The statistical error on the DOAS fit (1-sigma SD), a direct output of the DOAS analysis, represents error source (1). Representative absolute values for σ_{DSCD} at minimum SZA around noon and high SZA at 80°, are typically in the order of 3.4×10^{14} and 5.5×10^{14} molec cm^{-2}, respectively. As described in Sect. 3.1, the retrieved NO_2 DSCDs are quality-checked for outliers and those are filtered out, prior to further processing.

Error source (2) is the uncertainty related to the statistical Minimum-amount Langley-Extrapolation method utilized for the determination of the residual amount in the reference spectrum. The RMS error on the fit is estimated to be 1.3×10^{15} molec cm^{-2}.

As described in Sect. 3.4, different steps are involved in the determination of the stratospheric abundance, all contributing to the overall SSCD error (error source 3). The corresponding error sources can be summed in quadrature to obtain an estimate for σ_{SSCD} and are the following:

i. A first main error source originates from the retrieval approach of stratospheric VCDs at 90° SZA at sunrise and sunset. As the air mass, which is sampled at twilight, might be several hundred kilometers further away towards the sun, the effective SZA at the location of the air mass is lower than the 90° SZA at the measurement station, used so far in the standard NDACC retrieval. To take this effect into account, stratospheric VCDs have been also retrieved at 87° SZA at sunrise and sunset and the impact on the tropospheric VCDs has been investigated. The retrieved stratospheric VCDs corresponding to 87° SZA are approximately 3.7×10^{14} molec cm^{-2} lower than at 90° SZA. This causes an average increase of the retrieved tropospheric VCDs of 5 %.

ii. A second uncertainty comes from the error in the simulation of the NO_2 diurnal cycle by the stacked box photochemical model and the assimilation with the retrieved stratospheric VCDs at sunrise and sunset. Previous sensitivity studies taking into account uncertainties related to NO_x partitioning reaction rates, O_3 and temperature profiles, and aerosol loading pointed out that 20 % is a conser-

Discussion Paper | Discussion Paper | Discussion Paper | Discussion Paper |

AMTD

8, 935–985, 2015

Tropospheric NO_2 column retrieval from ground-based zenith-sky DOAS observations

F. Tack et al.

vative value for the uncertainty on modeled stratospheric NO_2 VCDs and profiles (Preston et al., 1997; Bracher et al., 2005).

iii. The third main error source is the uncertainty on the stratospheric AMFs, which is mainly due to the choice of the RT model settings. Several studies (e.g. Solomon et al., 1987; Van Roozendael et al., 1994; Ionov et al., 2008) showed that this uncertainty is of about 10 % at 90° SZA.

iv. The fourth error source, contributing to the overall SSCD error, results from the selection of a fixed reference day to determine the stratospheric content and the assumption of temporal invariance of stratospheric NO_2. Although the variation of the stratospheric NO_2 content is small at mid-latitude in summer over a short time interval, like the duration of the CINDI campaign, this error is taken into account by estimating the maximal variation between the simulations of the NO_2 diurnal cycle for all days of the acquisition period. This uncertainty is found to be approximately of 1.8×10^{14} molec cm^{-2}.

Errors in the calculation of the tropospheric AMFs, due to uncertainties in the RT model parameters, are the major error source (4). They affect the retrievals in a systematic way. In Chen et al. (2009) and Wang et al. (2012), a thorough sensitivity study is applied with varying input parameters in the radiative transfer simulations. The influence of parameters such as aerosol and NO_2 layer height, aerosol optical depth (AOD) and NO_2 profile, surface albedo, etc. has been tested. Based on these sensitivity studies, the uncertainty on TAMF is estimated to range between 10 and 20 % for SZAs between 20 and 85°. As in our retrieval approach daily NO_2 and aerosol profiles, retrieved from the MAX-DOAS observations, were utilised instead of model data for the a priori profile shape, it is assumed that σ_{TAMF} should be definitely within the estimated uncertainties. This is confirmed by the estimation of the uncertainty on the AMFs due to the variability of the NO_2 vertical profiles retrieved during CINDI, which is found to be of 12 % on average.

Discussion Paper | Discussion Paper | Discussion Paper | Discussion Paper |

AMTD
8, 935–985, 2015

Tropospheric NO_2 column retrieval from ground-based zenith-sky DOAS observations

F. Tack et al.

Results of the error budget analysis are summarised in Table 2 and are visualised in Fig. 5. In Table 2, the typical relative errors are presented according to the observed tropospheric NO_2 amount: (1) low (below 33th percentile or $< 0.6 \times 10^{16}$ molec cm^{-2}), (2) moderate (between 33th and 66th percentile or 0.6 and 1.0×10^{16} molec cm^{-2}), and (3) high (above 66th percentile or $> 1.0 \times 10^{16}$ molec cm^{-2}) NO_2 TVCD values. For each NO_2 TVCD range, the mean relative uncertainty σ is given for both the individual main error sources and the corresponding overall errors.

The error budget indicates that the overall uncertainty σ_{TVCD} on the retrieved NO_2 TVCDs is on average of 28 %. Larger errors (~ 40 %) are obtained in case of small TVCD values. In this case, the errors are dominated by uncertainties in the determination of the NO_2 SCD residual amount in the reference spectrum. For moderate and high TVCD values, the corresponding overall relative errors are of 24 and 21 % respectively. In these conditions, the main error sources are the determination of the stratospheric NO_2 abundance and the calculation of tropospheric AMFs. Errors related to the DOAS retrieval (σ_{DSCD}) and to the determination of the residual amount (σ_{RSCD}) seem to drop in case of larger NO_2 TVCDs, while errors originating from the determination of the stratospheric NO_2 abundance (σ_{SSCD}) are not depending significantly on the TVCD values. Errors due to the calculation of tropospheric AMFs (σ_{TAMF}), on the other hand, slightly increase with increasing TVCDs. In Fig. 5 the estimated overall absolute and relative errors are plotted in function of the retrieved NO_2 TVCDs. It can be seen that the largest absolute errors are associated with the largest TVCD values as expected. The relative errors, on the other hand, which can be up to 100 % in case of very low tropospheric contributions show a steep and rapid drop in case of increasing TVCDs. The relative error is almost constant (~ 22 %) for NO_2 TVCDs larger than 2.0×10^{16} molec cm^{-2}.

AMTD
8, 935–985, 2015

4 Retrieval results – correlative comparison

The tropospheric NO_2 columns have been compared with correlative datasets in order to thoroughly assess our ZS retrieval algorithm. To ensure comparability of data, and to reduce instrumental and algorithmic differences, a set of measurement requirements were defined in the framework of CINDI, which had to be performed by all instruments to the greatest possible extent (Piters el al., 2012). The same holds for the parameter settings for the trace gas retrieval as well as the relevant cross-sections included in the spectral fit (Roscoe et al., 2010). A first comparison is done with the VCDs obtained from a SAOZ instrument, which has been operated during the CINDI campaign in the close proximity of the BIRA-IASB instrument. Then the retrieval results are compared with VCDs from MAX-DOAS and DS-DOAS observations, also performed with the BIRA-IASB instrument.

4.1 ZS-DOAS SAOZ

The ZS-DOAS SAOZ instrument has been developed by CNRS-LATMOS at the end of 1980's. Since then, about 20 SAOZ instruments have been installed at various latitudes on the globe with initially the measurement of stratospheric ozone and NO_2 as main objective. Instrumental set-up has been described in Pommereau and Goutail (1998) and Piters et al. (2012) for the CINDI campaign. During the CINDI campaign, a measurement was done every 2 min, resulting in a high frequency of ZS observations. The retrieval strategy is discussed in Dieudonné et al. (2013).

4.2 MAX-DOAS

In addition to zenith-sky observations, the BIRA-IASB MAX-DOAS instrument measured scattered sunlight at different elevation angles towards the horizon, hereby increasing the sensitivity to absorbers present close to the ground. The azimuth was fixed along a west-north-westerly direction (287°) with an unobstructed view down to

AMTD
8, 935–985, 2015

an elevation angle of 0.5°. Tropospheric NO_2 vertical profiles and corresponding VCDs have been retrieved by applying the bePRO profiling tool (Clémer et al., 2010; Hendrick et al., 2014) to the measured off-axis DSCDs. Retrieval settings are described in Sect. 3.2.2.

4.3 DS-DOAS

The BIRA-IASB instrument is also able to perform observations of direct solar irradiance. NO_2 vertical columns can be accurately retrieved based on the DS-DOAS approach as the light path through the atmosphere, and subsequently the AMF, is straightforward to model. The determination of the AMF does not require complex radiative transfer calculations, but can be geometrically derived as the secant of the SZA. This significantly reduces uncertainties in the conversion from slant to vertical columns. The stratospheric contribution, determined as described in Sect. 3.4, is subtracted from the total NO_2 columns in order to obtain tropospheric VCDs. A major drawback of the DS observation is the dependency on clear-sky conditions. As cloud cover was substantial during the CINDI campaign, the acquired DS-DOAS dataset is relatively scarce. The fundamentals of DS-DOAS are extensively discussed in Brewer et al. (1973), Cede et al. (2006), and Herman et al. (2009).

4.4 Discussion of the correlative comparison

The comparisons between ZS-DOAS and SAOZ, ZS-DOAS and MAX-DOAS, and ZS-DOAS and DS-DOAS are shown in Fig. 6. A complete scan with the BIRA-IASB instrument, consisting of ten off-axis measurements at different elevation angles including zenith takes approximately 20 min of measurement time. The frequency of ZS measurements is therefore much lower than in case of the SAOZ, which is an instrument dedicated to perform only ZS observations (approximately one measurement every two minutes). To reduce the temporal variability due to different measurement sampling and to intercompare the different datasets in a meaningful way, the retrievals are averaged

Discussion Paper | Discussion Paper | Discussion Paper | Discussion Paper |

AMTD

8, 935–985, 2015

Tropospheric NO_2 column retrieval from ground-based zenith-sky DOAS observations

F. Tack et al.

in 30 min bins. An overall good agreement can be observed between ZS-DOAS, SAOZ, MAX-DOAS and DS-DOAS during the CINDI campaign, demonstrating the robustness and reliability of the presented approach.

Figure 7 shows the scatterplot and linear regression analysis of the binned and averaged NO_2 TVCDs, retrieved for the whole time series from (a) ZS-DOAS vs. SAOZ, and (b) ZS-DOAS vs. MAX-DOAS, respectively. For both comparisons a correlation coefficient higher than 0.9 can be observed. The linear regression analysis shows slopes within 18 % of unity and intercepts close to zero. In case of small NO_2 TVCD retrievals, we see a positive bias for the SAOZ with respect to ZS-DOAS retrievals, while the bias gets negative at higher TVCD values.

In Fig. 8 the NO_2 TVCD daily mean time series, retrieved from (a) ZS-DOAS and SAOZ, and (b) ZS-DOAS and MAX-DOAS, respectively, are compared. A very good consistency can be observed between the ZS-DOAS and SAOZ NO_2 TVCD retrievals, for both low and high TVCD values. The MAX-DOAS retrievals show similar day-to-day variations with respect to the ZS-DOAS and SAOZ retrievals. However, a positive bias of about 18 % on average can be observed for MAX-DOAS retrievals.

The same feature can be seen in Fig. 9, showing the retrieved NO_2 TVCD diurnal cycle of two subsequent days in the dataset, i.e. 3 July 2009 (day 184; see Fig. 9a) and 4 July 2009 (day 185; see Fig. 9b). For most retrievals, MAX-DOAS data shows a positive offset while DS-DOAS and SAOZ retrievals are very close to each other. This could be explained by the fact that different air masses were observed because of the different viewing geometries of the multi-axis and zenith-sky approach. It should also be noted that MAX-DOAS has a higher sensitivity to NO_2 present close to the ground than the other techniques. In Fig. 9, also the DS-DOAS retrievals are plotted. To avoid smoothing due to interpolation between the limited number of retrievals and for a better interpretation of the results, DS-DOAS retrievals are represented as point data. The DS-DOAS retrievals are seen to be in good agreement with the TVCDs retrieved by the other approaches.

AMTD
8, 935–985, 2015

It is clear from the observations that day to day tropospheric NO_2 concentrations can have a high variability at the Cabauw site. For day 184 (3 July), many tropospheric NO_2 pollution events can be observed. On the other hand, day 185 (4 July) is a clean day with low tropospheric NO_2 values, showing a smooth decrease in the morning and a slow build-up starting from noon. The meteorological parameters have shown that the NO_2 concentration variability is strongly depending on wind direction. On day 184, there were moderate winds ($4.3\,m\,s^{-1}$) from the southwest. The regions north of Cabauw are relatively clean, while there are strong pollution sources in the west (Rotterdam) and the south (industrial Flanders). When the wind is blowing from the south or west, retrievals from the Ozone Monitoring Instrument (OMI) as well as CHIMERE simulations over Cabauw have shown tropospheric NO_2 columns that are approximately two times higher than on days with winds from the north or east (Piters et al., 2012). On day 185 there was a light breeze ($2.5\,m\,s^{-1}$) from the northwest. On this day, the air over Cabauw was dominated by cleaner air originating from the North Sea.

5 Discussion and recommendations

In this section, the presented retrieval approach is briefly discussed with a focus on recommendations to improve the applicability on ZS observations acquired at other GB stations. From the error budget analysis can be concluded that reliable NO_2 TVCDs can be retrieved in case of moderate and strong polluted sites. Cabauw is a typical example of such a site as it is a semi-rural area, in the direct proximity of the four largest cities of the Netherlands. Depending on the meteorological conditions, the city may therefore be subject to substantial pollution events. In case of application of the retrieval approach on ZS observations performed at a station with very low or very high tropospheric content, some recommendations are made below.

Application of chemically-modified Langley plots (Lee et al., 1994), which are frequently used for determination of the NO_2 residual amount in the reference spectrum, was meaningless in case of the Cabauw dataset. Only the observations in a limited

Discussion Paper | Discussion Paper | Discussion Paper | Discussion Paper |
AMTD
8, 935–985, 2015
Tropospheric NO_2 column retrieval from ground-based zenith-sky DOAS observations
F. Tack et al.

SZA range (90–80°) with low tropospheric sensitivity could be used, since tropospheric pollution events can affect the straight-line fits of the Langley plot method. Along with the low frequency of ZS observations, i.e. each 15 to 20 min, too few data points remained in the plot to be statistically relevant. Furthermore, some tropospheric contamination could still be observed, even at high SZA. Constantin et al. (2013) reported similar issues with the chemically-modified Langley plot method, when applied on observations from a polluted site. For the selection of the SZA interval, a trade-off was discussed between having a sufficiently large set of observations while avoiding tropospheric contamination at lower SZA. In case of low to moderate tropospheric content, it is however strongly recommended to apply both the MLE and the chemically-modified Langley plot methods in order to further constrain the determination of the residual amount in the reference spectrum and to reduce the substantial uncertainties in this step.

Another important error source is the determination of the stratospheric contribution. The assumption that the tropospheric contribution is negligible in case of ZS observations at dawn and dusk does not always count in case of sites where frequent strong pollution events occur. Therefore, an approach was proposed to identify a non-polluted reference day and to assume that the retrieved stratospheric content for this day is representative for the whole dataset. It is recommended, however, to use daily observations (or to take a weekly mean) of the stratospheric NO_2 amount in the absence of frequent tropospheric pollution events in order to reduce the uncertainties introduced by the temporal variance and/or seasonality of the stratospheric NO_2 content.

In Chen et al. (2009) a strategy was applied to determine the stratospheric contribution in case of a heavy polluted site. Due to severe tropospheric contamination at the measurement site in Shanghai (China), no clean reference day could be identified in the dataset. Instead, measurements were done at Chongming Island, which lies to the northeast of Shanghai in the Pacific Ocean. Chongming can be considered as the area with the smallest tropospheric NO_2 pollution in the proximity of Shanghai. The SVCDs determined for a clean day at Chongming Island were eventually used to retrieve the

AMTD
8, 935–985, 2015

TVCDs from the observations acquired in Shanghai. This strategy can be, however, an additional error source, because of the spatial and temporal variations of the stratospheric NO_2 content. It makes also difficult its application to any other station due to the need of these additional measurements in a clean site.

6 Application at the NDACC site OHP

The potential of the presented ZS retrieval algorithm is also demonstrated by its application on observations acquired at the NDACC station Observatoire de Haute Provence (OHP, 43.94° N, 5.71° E, ~ 650 m a.s.l.), where BIRA-IASB and LATMOS operate a MAX-DOAS (UV channel only) and a SAOZ instrument, respectively. OHP is a mostly remote site at mid-latitude in Southern France, affected from time to time by pollution events coming from the Marseille area (South of OHP). Tropospheric columns are retrieved for a 2 year period from August 2012 to July 2014.

Taken the recommendations of Sect. 5 into account, slightly different strategies are applied in the different steps of the retrieval approach: (1) For the determination of the RSCD, the comparison between the chemically-modified Langley plot and the MLE method shows consistent results when applied on observations acquired at a background station like OHP. Both a higher frequency of ZS observations and the lack of frequent tropospheric contamination results in a sufficiently large and reliable dataset to derive the RSCD by linear least-squares regression in the chemically-modified Langley plot. A single noon spectrum, selected on 31 August 2013 at 11:40 LT, is used for the analysis of the whole time series. For the RSCD, a value of 2.7×10^{15} molec cm^{-2} is determined. (2) Due to the absence of frequent tropospheric pollution events at twilight, daily observations of the stratospheric contribution could be performed instead of retrieving the stratospheric content for a number of reference days, representative for parts of the dataset. This strategy reduces the uncertainties introduced by the temporal variance and/or seasonality of the stratospheric NO_2 content. (3) A seasonally-resolved climatology of tropospheric NO_2 AMFs has been generated based on the

AMTD
8, 935–985, 2015

Tropospheric NO_2 column retrieval from ground-based zenith-sky DOAS observations

F. Tack et al.

lower tropospheric NO_2 vertical profiles retrieved by applying the bePRO algorithm (see Sect. 3.2.2) to the August 2012 to July 2014 MAX-DOAS measurements at OHP. At this station, the MAX-DOAS instrument operates only in the UV at the following elevation angles: 2, 4, 6, 8, 11, 26, and 90° (zenith). Regarding the a priori NO_2 profiles, exponentially decreasing profiles corresponding to the vertical columns determined by the geometrical approximation and a scaling height of 0.5 km has been chosen. In the case of aerosol retrievals, a single extinction profile taken from the LOWTRAN climatology and corresponding to background conditions has been used as a priori. The retrieval altitude grid is one layer of 150 m thickness between 0.65 (altitude of the station) and 0.8 km altitude, 10 layers of 200 m thickness between 0.8 and 3 km, and one layer of 1 km thickness between 3 and 4 km. NO_2 and aerosol extinction profiles have been retrieved at 370 and 360 nm, respectively. In the case of AMF calculation, the following wavelength were selected: 370 and 460 nm. These two sets of UV and visible AMFs have been used for the application of the ZS approach to the MAX-DOAS and SAOZ measurements, respectively. For the calculation of AMFs in the visible, the aerosol profiles retrieved at 360 nm have been converted to 460 nm using the Ångström exponents derived from collocated CIMEL/AERONET sun photometer measurements (http://aeronet.gsfc.nasa.gov; see also Wang et al., 2014). MAX-DOAS NO_2 vertical columns involved in the comparison with the ZS method have been derived by integrating the retrieved NO_2 vertical profiles.

The retrieved TVCDs have been compared again with correlative datasets from SAOZ and MAX-DOAS observations and the resulting monthly mean time series are shown in Fig. 10. At OHP, a marked seasonal cycle can be observed with a maximum in winter with mean values close to 3×10^{15} molec cm^{-2} and a minimum in summer with mean values around 1.7×10^{15} molec cm^{-2}. In general the three datasets are in good agreement for both low and high TVCDs: the correlation coefficients are respectively 0.82 and 0.88 for the comparison of ZS-DOAS with MAX-DOAS and with SAOZ. These results further support the good reliability of the ZS retrieval approach presented in this study.

AMTD
8, 935–985, 2015

7 Summary and conclusions

An algorithm for retrieving tropospheric NO_2 VCDs from GB ZS DOAS measurements has been presented, with a full characterisation of the different retrieval steps. This algorithm has been developed and tested based on ZS observations from the BIRA-IASB MAX-DOAS instrument, acquired during the CINDI campaign at Cabauw, the Netherlands. For the tropospheric VCDs, a median value of 7.9×10^{15} molec cm^{-2} can be observed at the Cabauw site with maxima up to 6.0×10^{16} molec cm^{-2}. The retrievals are in good agreement when compared to TVCDs retrieved from off-axis and DS observations, and ZS measurements acquired by a co-located SAOZ instrument. For both comparisons a correlation higher than 0.9 can be observed with slopes within 18 % of unity and intercepts close to zero. The main error sources are characterised for the four principal steps of the retrieval approach:

1. Uncertainties due to the DOAS analysis and noise in the spectral measurements result in a relative error of approximately 14 and 3 % for low and high tropospheric VCD retrievals, respectively. It should be noted that DSCDs are quality-checked, including the removal of outliers, and compensated for multiple scattering events prior to the retrieval.

2. The NO_2 SCD residual amount in the fixed reference spectrum, measured on a non-polluted, clear-sky day around local noon, is determined based on the statistical Minimum-amount Langley-Extrapolation method. The related uncertainty can be substantial (22 % on average and up to 40 % in case of low NO_2 TVCDs). However, since a single RSCD is used for the analysis of the whole dataset, potential errors scarcely affect the relative variation of the retrieved tropospheric VCDs.

3. The stratospheric contribution to the total column is determined based on a two-step approach. First, stratospheric VCDs are retrieved for both 90° SZA sunrise and sunset for the selected reference day (23 June 2009). Then the NO_2 diurnal

AMTD
8, 935–985, 2015

variation between the 90° SZA twilight observations, modeled by the photochemical box-model PSCBOX, is fitted to these observations. The overall error for this step is estimated to be around 19 %. It accounts for the uncertainties due to (1) the determination of the effective SZA corresponding to the twilight observations, (2) the modeling of the NO_2 diurnal variation, (3) the simulation of stratospheric AMFs, and (4) the assumption of the temporal invariance of stratospheric NO_2 during the CINDI campaign period.

4. In the last step of the retrieval approach, tropospheric NO_2 slant columns retrieved between 80° SZA sunrise and sunset are converted to vertical columns by using appropriate tropospheric AMFs. Errors on the calculation of the tropospheric AMFs are estimated to range between 10 and 20 %, depending on the SZA.

In general, the error budget analysis indicates that tropospheric NO_2 VCDs can be retrieved with the ZS approach with an uncertainty σ_{TVCD} of less than 28 %. In case of low tropospheric content, the relative errors are found to be higher (i.e. in the order of 40 %) and are dominated by uncertainties in the determination of the residual amount in the reference spectrum. In case of strong tropospheric pollution events, the overall error drops to approximately 22 %. So the TVCD retrievals are generally more reliable in case of large tropospheric contributions, as expected, and for such conditions, the largest uncertainties find their origins in the determination of the stratospheric NO_2 abundance (19 %) and the calculation of tropospheric AMFs (15 %).

The present study demonstrates that ZS observations, widely used for monitoring of the stratospheric composition since about three decades, are also suitable for the retrieval of tropospheric NO_2 column amounts, despite the lower sensitivity to the troposphere when compared to MAX-DOAS observations. In order to further demonstrate the potential of the presented retrieval algorithm, it has been successfully applied on a 2 year dataset acquired at OHP, being a background site from time to time affected by pollution events. This offers new perspectives for the exploitation of ZS UV-Vis ob-

AMTD
8, 935–985, 2015

servations at NDACC stations and the applicability of the algorithm on data from other stations as well as longer time series will be further investigated. At present, there are far more ZS-DOAS than MAX-DOAS GB stations at various latitudes and much longer time series of ZS observations are available than for MAX-DOAS, mainly due to the novelty of the latter technique. This makes the ZS retrieval approach relevant for investigating the long-term evolution of tropospheric NO_2, with a feed-back of more than two decades at some stations.

Acknowledgements. The CINDI Campaign was largely funded by the ESA project CEOS (ESRIN 22202/09/I-EC) and the EU project ACCENT-AT2 (GOCE-CT-2004-505337). We further acknowledge the support of the European Union Seventh Framework Programme via the NORS project (FP7-284421) and the ACTRIS project (FP7-262254). BIRA-IASB is also thankful for the support from the Belgian Federal Science Policy Office through the AGACC-II project (SD/CS/07A). M. P. Chipperfield, from the University of Leeds, is gratefully acknowledged for providing us with the SLIMCAT data. The team of LATMOS wishes to thank the French Centre National d'Etudes Spatiales (CNES) and Institut des Sciences de l'Univers (INSU). The authors also want to express their gratitude to the KNMI staff at Cabauw for their technical support and the offered infrastructure.

References

Beirle, S., Kühl, S., Puķīte, J., and Wagner, T.: Retrieval of tropospheric column densities of NO_2 from combined SCIAMACHY nadir/limb measurements, Atmos. Meas. Tech., 3, 283–299, doi:10.5194/amt-3-283-2010, 2010.

Berg, N., Mellqvist, J., Jalkanen, J.-P., and Balzani, J.: Ship emissions of SO_2 and NO_2: DOAS measurements from airborne platforms, Atmos. Meas. Tech., 5, 1085–1098, doi:10.5194/amt-5-1085-2012, 2012.

Boersma, K. F., Eskes, H. J., Dirksen, R. J., van der A, R. J., Veefkind, J. P., Stammes, P., Huijnen, V., Kleipool, Q. L., Sneep, M., Claas, J., Leitão, J., Richter, A., Zhou, Y., and Brunner, D.: An improved tropospheric NO_2 column retrieval algorithm for the Ozone Monitoring Instrument, Atmos. Meas. Tech., 4, 1905–1928, doi:10.5194/amt-4-1905-2011, 2011.

AMTD

8, 935–985, 2015

Tropospheric NO_2 column retrieval from ground-based zenith-sky DOAS observations

F. Tack et al.

Bogumil, K., Orphal, J., Homann, T., Voigt, S., Spietz, P., Fleischmann, O. C., Vogel, A., Hartmann, M., Bovensmann, H., Frerik, J., and Burrows, J. P.: Measurements of molecular absorption spectra with the SCIAMACHY Pre-Flight Model: instrument characterization and reference spectra for atmospheric remote sensing in the 230–2380 nm region, J. Photoch. Photobio. A, 157, 167–184, 2003.
Bracher, A., Sinnhuber, M., Rozanov, A., and Burrows, J. P.: Using a photochemical model for the validation of NO_2 satellite measurements at different solar zenith angles, Atmos. Chem. Phys., 5, 393–408, doi:10.5194/acp-5-393-2005, 2005.
Brewer, A. W., McElroy, C. T., and Kerr, J. B.: Nitrogen dioxide concentrations in the atmosphere, Nature, 246, 129–133, 1973.
Bucsela, E. J., Krotkov, N. A., Celarier, E. A., Lamsal, L. N., Swartz, W. H., Bhartia, P. K., Boersma, K. F., Veefkind, J. P., Gleason, J. F., and Pickering, K. E.: A new stratospheric and tropospheric NO_2 retrieval algorithm for nadir-viewing satellite instruments: applications to OMI, Atmos. Meas. Tech., 6, 2607–2626, doi:10.5194/amt-6-2607-2013, 2013.
Cede, A., Herman, J., Richter, A., Krotkov, N., and Burrows, J.: Measurements of nitrogen dioxide total column amounts at Goddard Space Flight Center using a Brewer spectrometer in direct sun mode, J. Geophys. Res., 111, D05304, doi:10.1029/2005JD006585, 2006.
Chan, A. W. H., Chan, M. N., Surratt, J. D., Chhabra, P. S., Loza, C. L., Crounse, J. D., Yee, L. D., Flagan, R. C., Wennberg, P. O., and Seinfeld, J. H.: Role of aldehyde chemistry and NO_x concentrations in secondary organic aerosol formation, Atmos. Chem. Phys., 10, 7169–7188, doi:10.5194/acp-10-7169-2010, 2010.
Chance, K. and Kurucz, R. L.: An improved high-resolution solar reference spectrum for Earth's atmosphere measurements in the ultraviolet, visible, and near infrared, available at: http://www.cfa.harvard.edu/atmosphere (last access: September 2013), 2010.
Chance, K. V. and Spurr, R. J. D.: Ring effect studies: rayleigh scattering, including molecular parameters for rotational Raman scattering, and the Fraunhofer spectrum, Appl. Optics, 36, 5224–5230, 1997.
Chen, D., Zhou, B., Beirle, S., Chen, L. M., and Wagner, T.: Tropospheric NO_2 column densities deduced from zenith-sky DOAS measurements in Shanghai, China, and their application to satellite validation, Atmos. Chem. Phys., 9, 3641–3662, doi:10.5194/acp-9-3641-2009, 2009.

Chipperfield, M. P.: New version of the TOMCAT/SLIMCAT off-line chemical transport model: intercomparison of stratospheric tracer experiments, Q. J. Roy. Meteor. Soc., 132, 1179–1203, doi:10.1256/qj.05.51, 2006.

Clémer, K., Van Roozendael, M., Fayt, C., Hendrick, F., Hermans, C., Pinardi, G., Spurr, R., Wang, P., and De Mazière, M.: Multiple wavelength retrieval of tropospheric aerosol optical properties from MAXDOAS measurements in Beijing, Atmos. Meas. Tech., 3, 863–878, doi:10.5194/amt-3-863-2010, 2010.

Constantin, D.-E., Merlaud, A., Van Roozendael, M., Voiculescu, M., Fayt, C., Hendrick, F., Pinardi, G., and Georgescu, L.: Measurements of tropospheric NO_2 in Romania using a zenith-sky mobile DOAS system and comparisons with satellite observations, Sensors, 13, 3922–3940, doi:10.3390/s130303922, 2013.

Crutzen, P.: The influence of nitrogen oxides on the atmospheric ozone content, Q. J. Roy. Meteor. Soc., 96, 320–325, 1970.

Crutzen, P. J.: The role of NO and NO_2 in the chemistry of the troposphere and stratosphere, Annu. Rev. Earth Pl. Sc., 7, 443–472, 1979.

Danckaert, T., Fayt, C., and Van Roozendael, M.: QDOAS software user manual 2.108, IASB/BIRA, Uccle, Belgium, 2014, available at http://uv-vis.aeronomie.be/software/QDOAS/QDOAS_manual.pdf (last access: 4 November 2014), 2014.

Denis, L., Roscoe, H. K., Chipperfield, M. P., Van Roozendael, M., and Goutail, F.: A new software suite for NO_2 vertical profile retrieval from ground-based zenith-sky spectrometers, J. Quant. Spectrosc. Ra., 92, 321–333, doi:10.1016/j.jqsrt.2004.07.030, 2005.

Dieudonné, E., Ravetta, F., Pelon, J., Goutail, F., and Pommereau, J. P.: Linking NO_2 surface concentration and integrated content in the urban developed atmospheric boundary layer, Geophys. Res. Lett., 40, 1247–1251, doi:10.1002/grl.50242, 2013.

Errera, Q. and Fonteyn, D.: Four-dimensional variational chemical assimilation of CRISTA stratospheric measurements, J. Geophys. Res., 106, 12253–12265, doi:10.1029/2001JD900010, 2001.

Frieß, U., Monks, P. S., Remedios, J. J., Rozanov, A., Sinreich, R., Wagner, T., and Platt, U.: MAX-DOAS O_4 measurements: a new technique to derive information on atmospheric aerosols: 2. Modeling studies, J. Geophys. Res., 111, D14203, doi:10.1029/2005JD006618, 2006.

Goutail, F., Pommereau, J.-P., and Sarkissian, A.: Total nitrogen dioxide at the Arctic Polar Circle since 1990, Geophys. Res. Lett., 21, 1371–740, 1994.

Grainger, J. F. and Ring, J.: Anomalous Fraunhofer line profiles, Nature, 193, p. 762, 1962.
Harder, J. W. and Brault, J. W.: Atmospheric measurements of water vapor in the 442-nm region, J. Geophys. Res., 102, 6245–6252, doi:10.1029/96JD01730, 1997.
Hendrick, F., Barret, B., Van Roozendael, M., Boesch, H., Butz, A., De Mazière, M., Goutail, F., Hermans, C., Lambert, J.-C., Pfeilsticker, K., and Pommereau, J.-P.: Retrieval of nitrogen dioxide stratospheric profiles from ground-based zenith-sky UV-visible observations: validation of the technique through correlative comparisons, Atmos. Chem. Phys., 4, 2091–2106, doi:10.5194/acp-4-2091-2004, 2004.
Hendrick, F., Van Roozendael, M., Kylling, A., Petritoli, A., Rozanov, A., Sanghavi, S., Schofield, R., von Friedeburg, C., Wagner, T., Wittrock, F., Fonteyn, D., and De Mazière, M.: Intercomparison exercise between different radiative transfer models used for the interpretation of ground-based zenith-sky and multi-axis DOAS observations, Atmos. Chem. Phys., 6, 93–108, doi:10.5194/acp-6-93-2006, 2006.
Hendrick, F., Müller, J.-F., Clémer, K., Wang, P., De Mazière, M., Fayt, C., Gielen, C., Hermans, C., Ma, J. Z., Pinardi, G., Stavrakou, T., Vlemmix, T., and Van Roozendael, M.: Four years of ground-based MAX-DOAS observations of HONO and NO_2 in the Beijing area, Atmos. Chem. Phys., 14, 765–781, doi:10.5194/acp-14-765-2014, 2014.
Herman, J., Cede, A., Spinei, E., Mount, G., Tzortziou, M., and Abuhassan, N.: NO_2 column amounts from ground-based Pandora and MFDOAS spectrometers using the direct-sun DOAS technique: intercomparisons and application to OMI validation, J. Geophys. Res., 114, D13307, doi:10.1029/2009JD011848, 2009.
Hermans, C., Vandaele, A. C., Fally, S., Carleer, M., Colin, R., Coquart, B., Jenouvrier, A., and Mérienne, M.-F.: Absorption cross-section of the collision-induced bands of oxygen from the UV to the NIR, in: Proceedings of the NATO Advanced Research Workshop, Weakly Interacting Molecular Pairs: Unconventional Absorbers of Radiation in the Atmosphere, Fontevraud, France, 24 April–2 May 2002, edited by: Camy-Peyret, C. and Vigasin, A. A., NATO Science Series IV Earth and Environmental Sciences, Vol. 27, Kluwer Academic Publishers, Boston, 193–202, 2003.
Hilboll, A., Richter, A., Rozanov, A., Hodnebrog, Ø., Heckel, A., Solberg, S., Stordal, F., and Burrows, J. P.: Improvements to the retrieval of tropospheric NO_2 from satellite – stratospheric correction using SCIAMACHY limb/nadir matching and comparison to Oslo CTM2 simulations, Atmos. Meas. Tech., 6, 565–584, doi:10.5194/amt-6-565-2013, 2013.

Hönninger, G., von Friedeburg, C., and Platt, U.: Multi axis differential optical absorption spectroscopy (MAX-DOAS), Atmos. Chem. Phys., 4, 231–254, doi:10.5194/acp-4-231-2004, 2004.
Ionov, D. V., Timofeyev, Y. M., Sinyakov, V. P., Semenov, V. K., Goutail, F., Pommereau, J.-P., Bucsela, E. J., Celarier, E. A., and Kroon, M.: Ground-based validation of EOS-Aura OMI NO_2 vertical column data in the midlatitude mountain ranges of Tien Shan (Kyrgyzstan) and Alps (France), J. Geophys. Res., 113, D15S08, doi:10.1029/2007JD008659, 2008.
Johansson, M., Rivera, C., de Foy, B., Lei, W., Song, J., Zhang, Y., Galle, B., and Molina, L.: Mobile mini-DOAS measurement of the outflow of NO_2 and HCHO from Mexico City, Atmos. Chem. Phys., 9, 5647–5653, doi:10.5194/acp-9-5647-2009, 2009.
Koelemeijer, R. B. A., de Haan, J. F., and Stammes, P.: A database of spectral surface reflectivity in the range 335–772 nm derived from 5.5 years of GOME observations, J. Geophys. Res., 108, 4070, doi:10.1029/2002JD002429, 2003.
Lee, A. M., Roscoe, H. K., Oldham, D. J., Squires, J. A. C., Sarkissian, A., and Pommereau, J.-P.: Improvements to the accuracy of zenith-sky measurements of NO_2 by visible spectrometers, J. Quant. Spectrosc. Ra., 52, 649–657, 1994.
Mayer, B. and Kylling, A.: Technical note: The libRadtran software package for radiative transfer calculations - description and examples of use, Atmos. Chem. Phys., 5, 1855–1877, doi:10.5194/acp-5-1855-2005, 2005.
McKenzie, R., Johnston, P. V., McElroy, C. T., Kerr, J. B., and Solomon, S.: Altitude distributions of stratospheric constituents from ground-based measurements at twilight, J. Geophys. Res., 96, 15499–15511, 1991.
Merlaud, A., Van Roozendael, M., van Gent, J., Fayt, C., Maes, J., Toledo-Fuentes, X., Ronveaux, O., and De Mazière, M.: DOAS measurements of NO_2 from an ultralight aircraft during the Earth Challenge expedition, Atmos. Meas. Tech., 5, 2057–2068, doi:10.5194/amt-5-2057-2012, 2012.
Noxon, J. F.: Nitrogen dioxide in the stratosphere and troposphere measured by ground-based absorption spectroscopy, Science, 189, 547–549, 1975.
Piters, A. J. M., Boersma, K. F., Kroon, M., Hains, J. C., Van Roozendael, M., Wittrock, F., Abuhassan, N., Adams, C., Akrami, M., Allaart, M. A. F., Apituley, A., Beirle, S., Bergwerff, J. B., Berkhout, A. J. C., Brunner, D., Cede, A., Chong, J., Clémer, K., Fayt, C., Frieß, U., Gast, L. F. L., Gil-Ojeda, M., Goutail, F., Graves, R., Griesfeller, A., Großmann, K., Hemerijckx, G., Hendrick, F., Henzing, B., Herman, J., Hermans, C., Hoexum, M., van der Hoff, G. R.,

AMTD
8, 935–985, 2015

Irie, H., Johnston, P. V., Kanaya, Y., Kim, Y. J., Klein Baltink, H., Kreher, K., de Leeuw, G., Leigh, R., Merlaud, A., Moerman, M. M., Monks, P. S., Mount, G. H., Navarro-Comas, M., Oetjen, H., Pazmino, A., Perez-Camacho, M., Peters, E., du Piesanie, A., Pinardi, G., Puentedura, O., Richter, A., Roscoe, H. K., Schönhardt, A., Schwarzenbach, B., Shaiganfar, R., Sluis, W., Spinei, E., Stolk, A. P., Strong, K., Swart, D. P. J., Takashima, H., Vlemmix, T., Vrekoussis, M., Wagner, T., Whyte, C., Wilson, K. M., Yela, M., Yilmaz, S., Zieger, P., and Zhou, Y.: The Cabauw Intercomparison campaign for Nitrogen Dioxide measuring Instruments (CINDI): design, execution, and early results, Atmos. Meas. Tech., 5, 457–485, doi:10.5194/amt-5-457-2012, 2012.

Platt, U.: Differential optical absorption spectroscopy (DOAS), in: Air Monitoring by Spectroscopic Techniques, 127, John Wiley & Sons, Hoboken, NJ, USA, 27–83, 1994.

Platt, U. and Stutz, J.: Differential Optical Absorption Spectroscopy: Principles and Applications, Springer-Verlag, Berlin, Germany, 2008.

Pommereau, J. P. and Goutail, F.: Stratospheric O_3 and NO_2 observations at the Southern Polar Circle in summer and fall 1988, Geophys. Res. Lett., 15, 895–897, doi:10.1029/GL015i008p00895, 1988.

Popp, C., Brunner, D., Damm, A., Van Roozendael, M., Fayt, C., and Buchmann, B.: High-resolution NO_2 remote sensing from the Airborne Prism EXperiment (APEX) imaging spectrometer, Atmos. Meas. Tech., 5, 2211–2225, doi:10.5194/amt-5-2211-2012, 2012.

Preston, K. E., Jones, R. L., and Roscoe, H. K.: Retrieval of NO_2 vertical profiles from ground-based UV-visible measurements: method and validation, J. Geophys. Res., 102, 10089–10097, 1997.

Richter, A. and Burrows, J. P.: Retrieval of tropospheric NO_2 from GOME measurements, Adv. Space Res., 29, 1673–1683, 2002.

Rodgers, C. D.: Inverse Methods for Atmospheric Sounding: Theory and Practice, Ser. Atmos. Oceanic Planet. Phys., Vol. 2, F. W. Taylor, World Sci., Hackensack, NY, USA, 2000.

Roscoe, H. K., Van Roozendael, M., Fayt, C., du Piesanie, A., Abuhassan, N., Adams, C., Akrami, M., Cede, A., Chong, J., Clémer, K., Friess, U., Gil Ojeda, M., Goutail, F., Graves, R., Griesfeller, A., Grossmann, K., Hemerijckx, G., Hendrick, F., Herman, J., Hermans, C., Irie, H., Johnston, P. V., Kanaya, Y., Kreher, K., Leigh, R., Merlaud, A., Mount, G. H., Navarro, M., Oetjen, H., Pazmino, A., Perez-Camacho, M., Peters, E., Pinardi, G., Puentedura, O., Richter, A., Schönhardt, A., Shaiganfar, R., Spinei, E., Strong, K., Takashima, H., Vlemmix, T., Vrekoussis, M., Wagner, T., Wittrock, F., Yela, M., Yilmaz, S., Boersma, F.,

AMTD
8, 935–985, 2015

Tropospheric NO_2 column retrieval from ground-based zenith-sky DOAS observations

F. Tack et al.

Hains, J., Kroon, M., Piters, A., and Kim, Y. J.: Intercomparison of slant column measurements of NO_2 and O_4 by MAX-DOAS and zenith-sky UV and visible spectrometers, Atmos. Meas. Tech., 3, 1629–1646, doi:10.5194/amt-3-1629-2010, 2010.

Solomon, S., Schmeltekopf, A. L., and Sanders, R. W.: On the interpretation of zenith sky measurements, J. Geophys. Res., 92, 8311–8319, doi:10.1029/JD092iD07p08311, 1987.

Solomon, S., Portmann, R. W., Sanders, R. W., Daniel, J. S., Madsen, W., Bartram, B., and Dutton, E. G.: On the role of nitrogen dioxide in the absorption of solar radiation, J. Geophys. Res., 104, 12047–12058, doi:10.1029/1999JD900035, 1999.

Spurr, R.: LIDORT and VLIDORT: Linearized pseudo-spherical scalar and vector discrete ordinate radiative transfer models for use in remote sensing retrieval problems, in: Light Scattering Reviews, edited by: Kokhanovsky, A., Vol. 3, Springer, 2008.

Valks, P., Pinardi, G., Richter, A., Lambert, J.-C., Hao, N., Loyola, D., Van Roozendael, M., and Emmadi, S.: Operational total and tropospheric NO_2 column retrieval for GOME-2, Atmos. Meas. Tech., 4, 1491–1514, doi:10.5194/amt-4-1491-2011, 2011.

Vandaele, A.-C., Hermans, C., Simon, P. C., Carleer, M., Colin, R., Fally, S., Mérienne, M.-F., Jenouvrier, A., and Coquart, B.: Measurements of the NO2 absorption cross-section from 42000 cm^{-1} to 10000 cm^{-1} (238–1000 nm) at 220 K and 294 K, J. Quant. Spectrosc. Ra., 59, 171–184, 1998.

Van Roozendael, M. and Hendrick, F.: Recommendations for NO_2 column retrieval from NDACC zenith-sky UV-VIS spectrometers, BIRA-IASB, Uccle, Belgium, 2012, available at: http://ndacc-uvvis-wg.aeronomie.be/tools/NDACC_UVVIS-WG_NO2settings_v4.pdf (last access: 24 October 2014), 2014.

Van Roozendael, M., De Mazière, M., and Simon, P. C.: Ground-based visible measurements at the Jungfraujoch station since 1990, J. Quant. Spectrosc. Ra., 52, 231–240, 1994.

Vlemmix, T., Piters, A. J. M., Berkhout, A. J. C., Gast, L. F. L., Wang, P., and Levelt, P. F.: Ability of the MAX-DOAS method to derive profile information for NO_2: can the boundary layer and free troposphere be separated?, Atmos. Meas. Tech., 4, 2659–2684, doi:10.5194/amt-4-2659-2011, 2011.

Wagner, T., Dix, B., Friedeburg, C. v., Frieß, U., Sanghavi, S., Sinreich, R., and Platt, U.: MAX-DOAS O_4 measurements: a new technique to derive information on atmospheric aerosols – principles and information content, J. Geophys. Res., 109, D22205, doi:10.1029/2004JD004904, 2004.

AMTD
8, 935–985, 2015

Wagner, T., Burrows, J. P., Deutschmann, T., Dix, B., von Friedeburg, C., Frieß, U., Hendrick, F., Heue, K.-P., Irie, H., Iwabuchi, H., Kanaya, Y., Keller, J., McLinden, C. A., Oetjen, H., Palazzi, E., Petritoli, A., Platt, U., Postylyakov, O., Pukite, J., Richter, A., van Roozendael, M., Rozanov, A., Rozanov, V., Sinreich, R., Sanghavi, S., and Wittrock, F.: Comparison of box-air-mass-factors and radiances for Multiple-Axis Differential Optical Absorption Spectroscopy (MAX-DOAS) geometries calculated from different UV/visible radiative transfer models, Atmos. Chem. Phys., 7, 1809–1833, doi:10.5194/acp-7-1809-2007, 2007.

Wagner, T., Ibrahim, O., Shaiganfar, R., and Platt, U.: Mobile MAX-DOAS observations of tropospheric trace gases, Atmos. Meas. Tech., 3, 129–140, doi:10.5194/amt-3-129-2010, 2010.

Wagner, T., Beirle, S., Brauers, T., Deutschmann, T., Frieß, U., Hak, C., Halla, J. D., Heue, K. P., Junkermann, W., Li, X., Platt, U., and Pundt-Gruber, I.: Inversion of tropospheric profiles of aerosol extinction and HCHO and NO_2 mixing ratios from MAX-DOAS observations in Milano during the summer of 2003 and comparison with independent data sets, Atmos. Meas. Tech., 4, 2685–2715, doi:10.5194/amt-4-2685-2011, 2011.

Wang, S., Zhou, B., Wang, Z., Yang, S., Hao, N., Valks, P., Trautmann, T., and Chen, L.: Remote sensing of NO_2 emission from the central urban area of Shanghai (China) using the mobile DOAS technique, J. Geophys. Res., 117, D13305, doi:10.1029/2011JD016983, 2012.

Wittrock, F., Oetjen, H., Richter, A., Fietkau, S., Medeke, T., Rozanov, A., and Burrows, J. P.: MAX-DOAS measurements of atmospheric trace gases in Ny-Ålesund – Radiative transfer studies and their application, Atmos. Chem. Phys., 4, 955–966, doi:10.5194/acp-4-955-2004, 2004.

World Health Organization: Review of Evidence on Health Aspects of Air Pollution (REVIHAAP) – Technical Report, WHO Regional Office for Europe, Copenhagen, Denmark, 302 pp., 2013.

AMTD

8, 935–985, 2015

Table 1. Main DOAS analysis parameter settings for NO_2 slant column spectral fit, in accordance with the NDACC UV-Vis Working Group recommendations (Van Roozendael and Hendrick, 2012).

Parameter	Settings
Fitting interval	425–490 nm
Wavelength calibration method	Calibration based on reference solar atlas (Chance and Kurucz, 2010)
Cross-sections	
NO_2	Vandaele et al. (1998), 298 K
O_3	Bogumil et al. (2003), 223 K
H_2O	Harder and Brault (1997)
O_4	Hermans et al. (2003)
Ring effect correction method	Chance and Spurr (1997)
Polynomial term	Polynomial of order 5
Intensity offset correction	Slope

AMTD
8, 935–985, 2015

Table 2. Error budget on the retrieved tropospheric NO_2 VCDs. The typical relative and absolute errors (in percent and 10^{15} molec cm^{-2}, respectively) are given for low (below 33th percentile or $< 0.6 \times 10^{16}$ molec cm^{-2}), moderate (between 33th and 66th percentile or 0.6 and 1.0×10^{16} molec cm^{-2}) and high (above 66th percentile or $> 1.0 \times 10^{16}$ molec cm^{-2}) NO_2 TVCD values, respectively. The last column gives the typical uncertainties on all retrieved TVCDs.

Error source	Low TVCD	Mod TVCD	High TVCD	Total TVCD
σ_{DSCD}	14 % (0.5)	6 % (0.4)	3 % (0.5)	8 % (0.5)
σ_{RSCD}	40 % (1.3)	16 % (1.3)	9 % (1.3)	22 % (1.3)
σ_{SSCD}	20 % (0.8)	19 % (1.5)	19 % (3.1)	19 % (1.8)
σ_{TAMF}	13 % (0.2)	14 % (0.2)	15 % (0.2)	14 % (0.2)
σ_{TVCD}	38 % (1.3)	24 % (1.9)	21 % (3.5)	28 % (2.2)

AMTD
8, 935–985, 2015

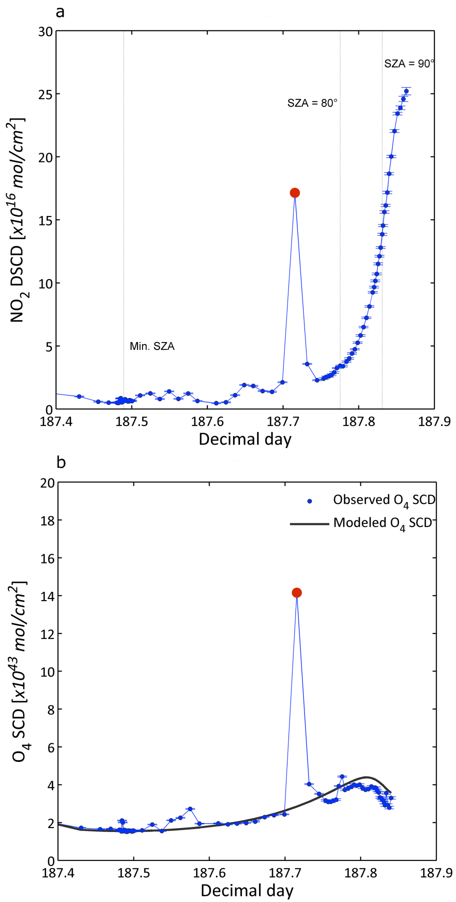

Figure 1. Example of a NO_2 enhancement event, due to multiple scattering, on day 187 (6 July 2009). Both **(a)** the NO_2 DSCD and **(b)** the O_4 SCD diurnal cycles show a large spike at approximately 17:10 LT (red dot).

AMTD
8, 935–985, 2015

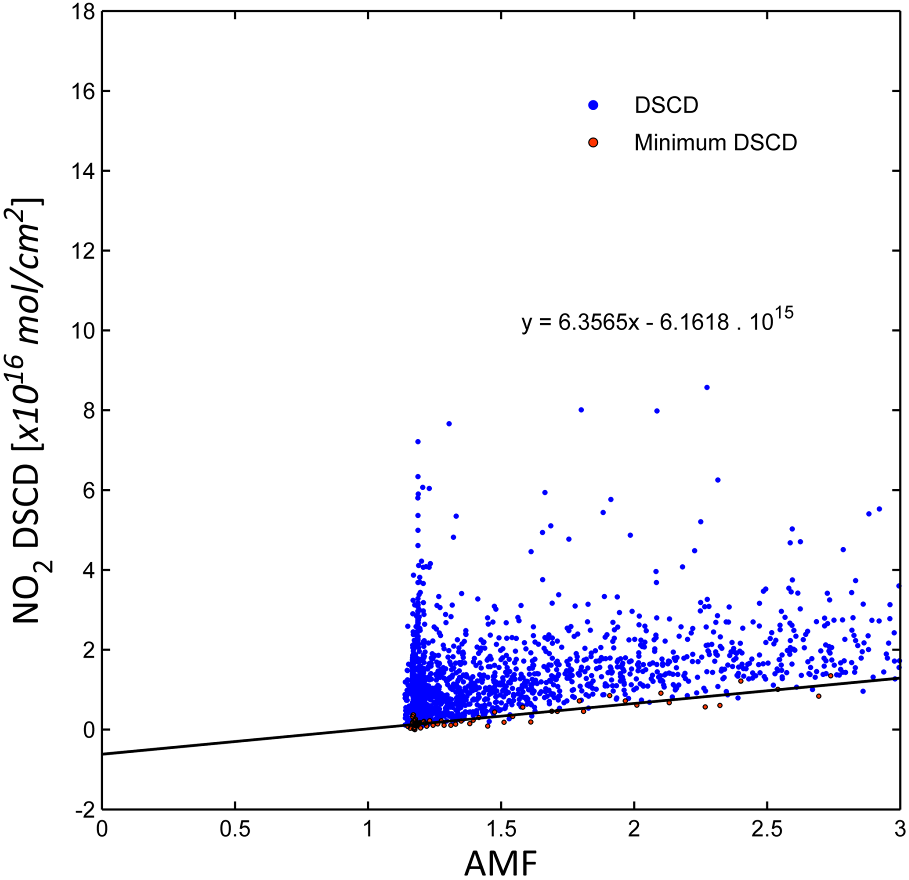

Figure 2. A value of 6.2×10^{15} molec cm^{-2} is determined for the residual amount in the reference spectrum (RSCD) based on application of the MLE method. The ZS noon spectrum was selected on 21 June 2009 at 12:16 LT.

AMTD
8, 935–985, 2015

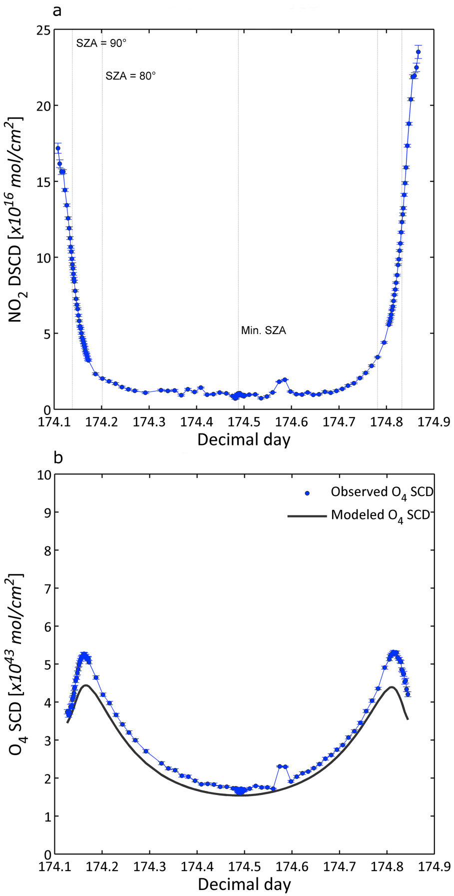

Figure 3. NO_2 and O_4 slant column diurnal cycle for the non-polluted, clear-sky reference day 174 (23 June 2009). **(a)** The NO_2 DSCD diurnal cycle, dominated by stratospheric absorption, has a typical u-shape with minimal tropospheric perturbations. **(b)** The observed O_4 SCD diurnal cycle largely follows the smooth curve, modeled with the RTM UVspec/DISORT.

AMTD
8, 935–985, 2015

Tropospheric NO_2 column retrieval from ground-based zenith-sky DOAS observations

F. Tack et al.

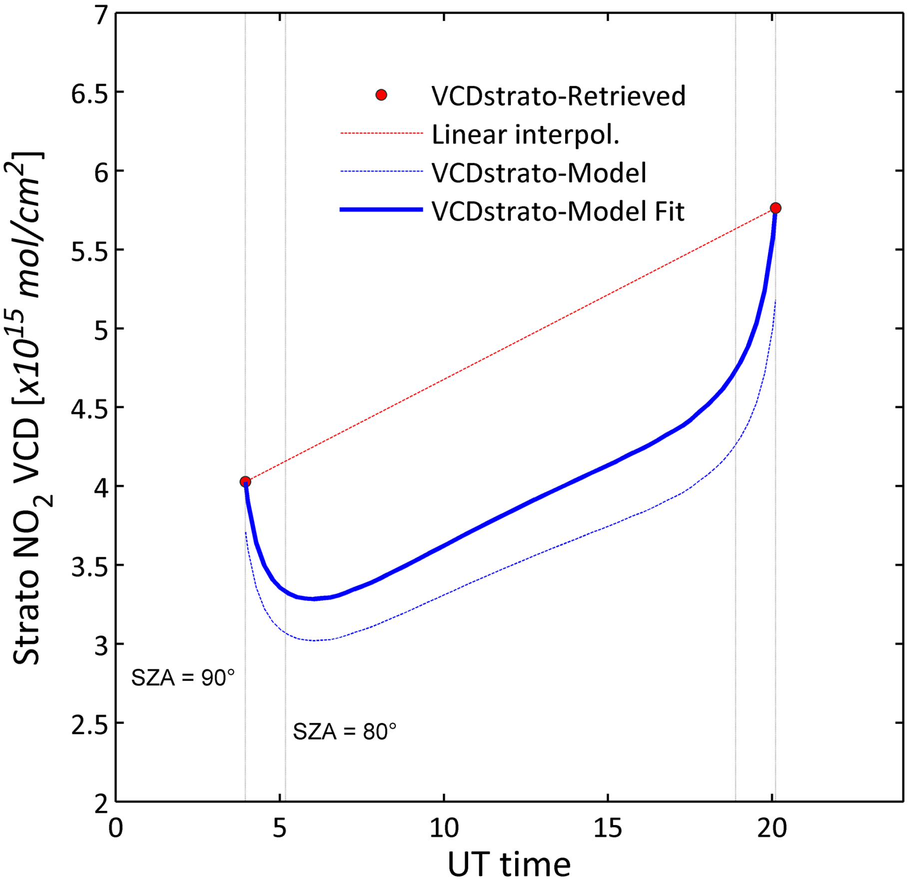

Figure 4. Representation of the retrieved stratospheric NO_2 VCDs at 90° SZA sunrise and sunset for reference day 174 (Sect. 3.4.1) and fit of the NO_2 diurnal cycle modeled with the photochemical model PSCBOX.

AMTD
8, 935–985, 2015

Tropospheric NO_2 column retrieval from ground-based zenith-sky DOAS observations

F. Tack et al.

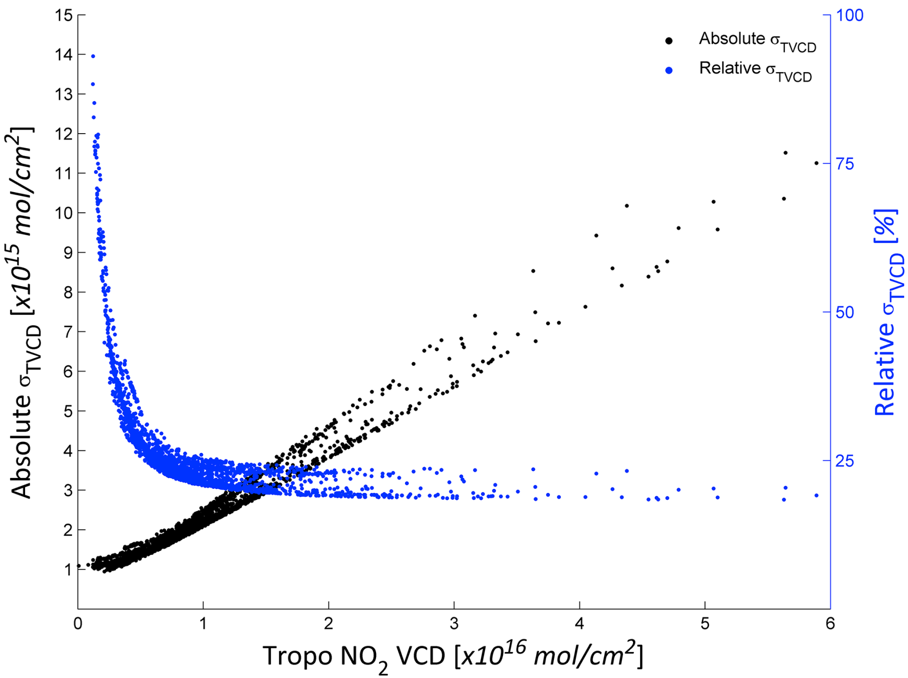

Figure 5. Overall absolute and relative errors (σ_{TVCD}) on the retrieved NO_2 TVCDs.

AMTD
8, 935–985, 2015

Tropospheric NO_2 column retrieval from ground-based zenith-sky DOAS observations

F. Tack et al.

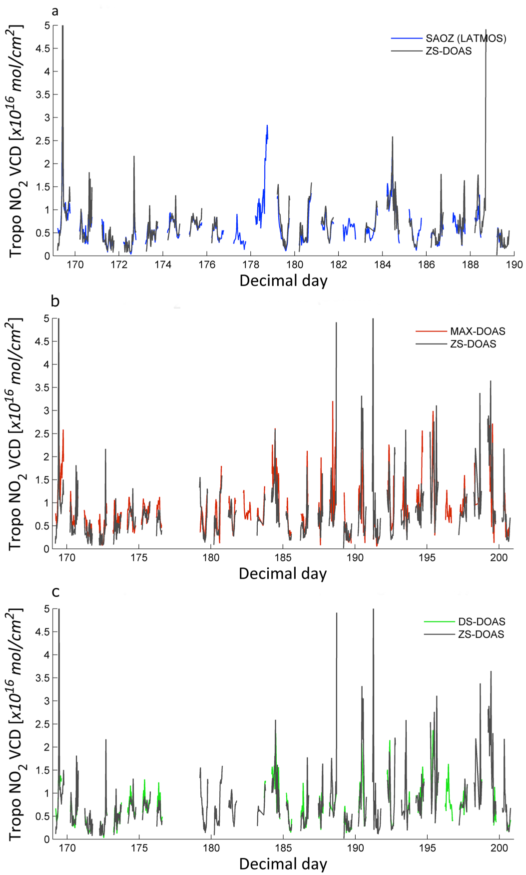

Figure 6. Comparisons of the tropospheric NO_2 VCD time series, between **(a)** ZS-DOAS and SAOZ, **(b)** ZS-DOAS and MAX-DOAS, and **(c)** ZS-DOAS and DS-DOAS. TVCDs are binned and averaged in timeslots of 30 min.

AMTD
8, 935–985, 2015

Tropospheric NO_2 column retrieval from ground-based zenith-sky DOAS observations

F. Tack et al.

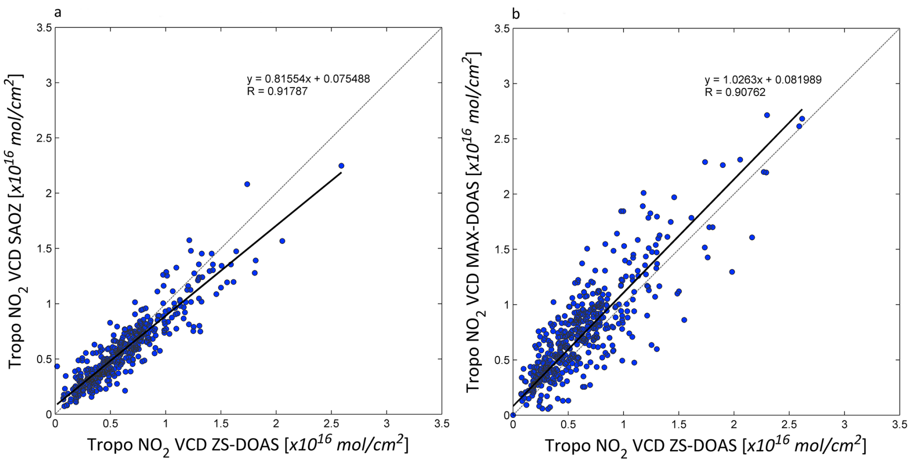

Figure 7. Scatter plot and linear regression analysis of the TVCDs retrieved for the whole time series from **(a)** ZS-DOAS and SAOZ, and **(b)** ZS-DOAS and MAX-DOAS, respectively. TVCDs are binned and averaged in 30 min bins.

AMTD
8, 935–985, 2015

Tropospheric NO_2 column retrieval from ground-based zenith-sky DOAS observations

F. Tack et al.

Title Page
Abstract | Introduction
Conclusions | References
Tables | Figures
◀| |▶
◀ ▶
Back | Close
Full Screen / Esc
Printer-friendly Version
Interactive Discussion

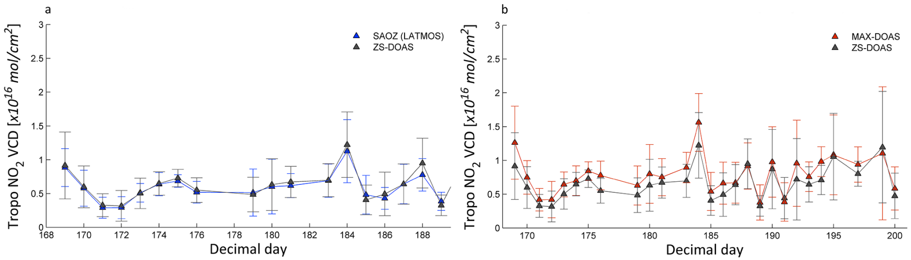

Figure 8. TVCD daily mean time series for **(a)** ZS-DOAS and SAOZ, and **(b)** ZS-DOAS and MAX-DOAS, respectively.

AMTD
8, 935–985, 2015

Tropospheric NO_2 column retrieval from ground-based zenith-sky DOAS observations

F. Tack et al.

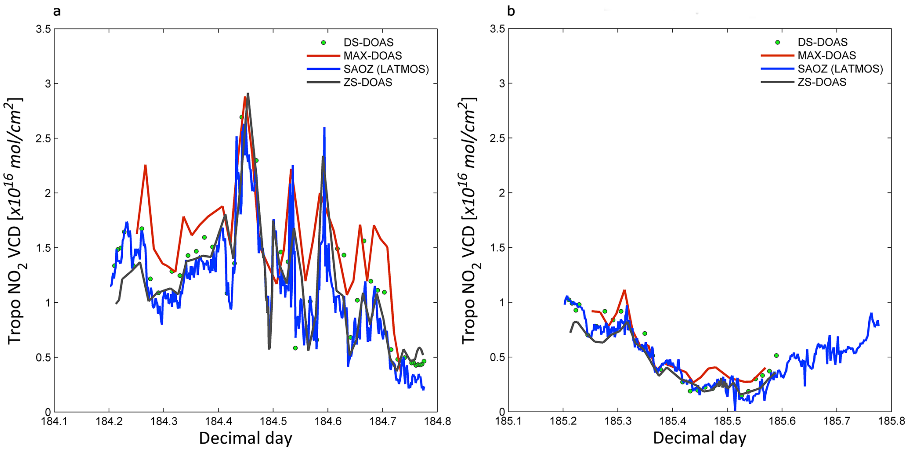

Figure 9. TVCD diurnal variation for **(a)** a day with many pollution events (day 184) and **(b)** a non-polluted day (185), respectively. To avoid smoothing due to interpolation between the limited number of retrievals and for a better interpretation of the results, DS-DOAS retrievals are represented as point data here.

AMTD
8, 935–985, 2015

Tropospheric NO_2 column retrieval from ground-based zenith-sky DOAS observations

F. Tack et al.

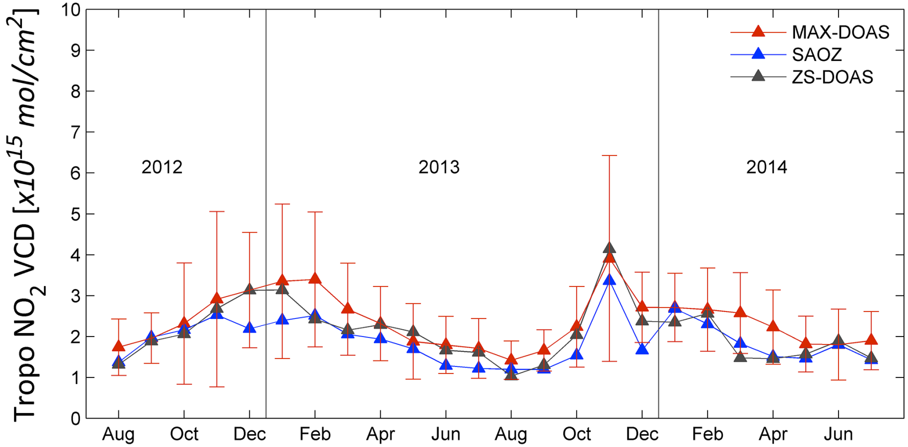

Figure 10. TVCD monthly mean time series at the OHP station for ZS-DOAS, SAOZ and MAX-DOAS for the period August 2012–July 2014. The error bars on the MAX-DOAS data points correspond to the one-sigma SD.